Report No. K-TRAN: KU-21-1 ▪ FINAL REPORT ▪ November 2024

Electric Vehicle Simulations Based on Kansas-Centric Conditions

Christopher Depcik, Ph.D.
Tyler Simpson
George Bousfield
Austin Wohleb

The University of Kansas

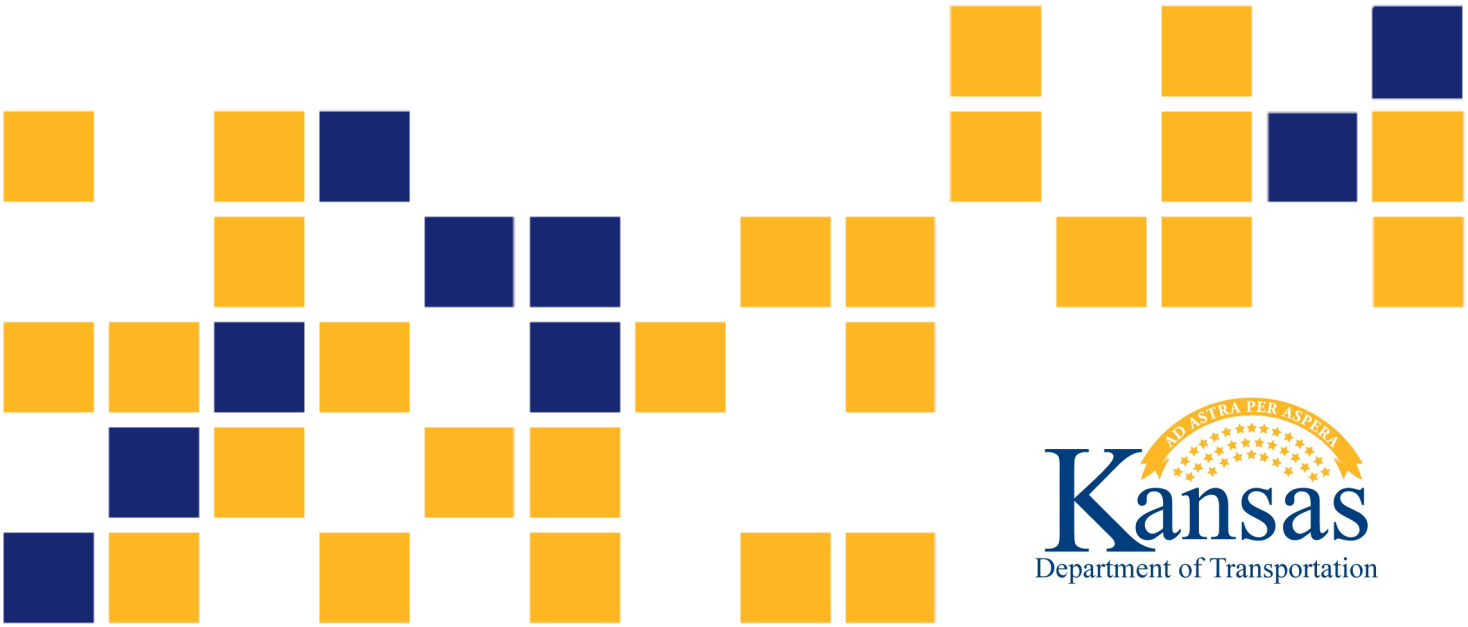

Kansas Department of Transportation

1 Report No. K-TRAN: KU-21-1	**2 Government Accession No.**	**3 Recipient Catalog No.**
4 Title and Subtitle Electric Vehicle Simulations Based on Kansas-Centric Conditions		**5 Report Date** November 2024 **6 Performing Organization Code**
7 Author(s) Christopher Depcik, Ph.D.; Tyler Simpson; George Bousfield; Austin Wohleb		**8 Performing Organization Report No.**
9 Performing Organization Name and Address The University of Kansas Department of Civil, Environmental & Architectural Engineering 1530 West 15th St Lawrence, Kansas 66045-7609		**10 Work Unit No. (TRAIS)** **11 Contract or Grant No.** C2168
12 Sponsoring Agency Name and Address Kansas Department of Transportation Bureau of Research 2300 SW Van Buren Topeka, Kansas 66611-1195		**13 Type of Report and Period Covered** Final Report July 2020 – June 2022 **14 Sponsoring Agency Code** RE-0813-01
15 Supplementary Notes For more information write to address in block 9.		

16 Abstract

Range anxiety is a significant contributor to consumer reticence when purchasing Electric Vehicles (EVs); thus, industry is pushing the range of EVs by enhancing lithium-ion battery chemistry. As a result, new commercial EVs readily achieve over 200 miles of range as found by the United States Environmental Protection Agency (EPA). However, this measured range by the EPA is often not the case when real-world conditions are encountered. The choice of testing indoors in idealized conditions (i.e., 77 ºF with the cabin conditioning system turned off) can belie the true range of EVs. This can be particularly problematic as government entities look to add charging stations nationwide. Any use of range that feeds into planning purposes must include on-road information such as wind (particularly important for the authors' home state of Kansas) and other facets like road grade and ambient temperature. Thus, this effort describes the simplest model that incorporates all important factors that impact the range of an EV. Calibration of the model to EPA tests found an average deviation of 0.45 and 0.57 miles for the highway and city ranges, respectively over seven commercial EVs; hence, demonstrating good model accuracy. Subsequent predictions found significant losses based on the impact of road grade, wind, and vehicle speed over a Kansas interstate highway. In addition, up to 57.8% and 37.5% losses in range were found when simulating vehicles at 20 ºF and 95 ºF, respectively. Simulated aging of the vehicle battery pack due to cycling demonstrated range losses up to 53.1% at 100,000 miles. Model extensions to rain and snow illustrated corresponding losses based on the level of precipitation on the road. Finally, all model outcomes were translated into simple Excel spreadsheets that can be used in predicting the range of a generic EV over Kansas-centric roads.

17 Key Words Electric Vehicles, Electric Vehicle Charging, Vehicle Range, Digital Simulation		**18 Distribution Statement** No restrictions. This document is available to the public through the National Technical Information Service www.ntis.gov.	
19 Security Classification (of this report) Unclassified	**20 Security Classification (of this page)** Unclassified	**21 No. of pages** 69	**22 Price**

Form DOT F 1700.7 (8-72)

This page intentionally left blank.

Electric Vehicle Simulations Based on Kansas-Centric Conditions

Final Report

Prepared by

Christopher Depcik, Ph.D.
Tyler Simpson
George Bousfield
Austin Wohleb

The University of Kansas

A Report on Research Sponsored by

THE KANSAS DEPARTMENT OF TRANSPORTATION
TOPEKA, KANSAS

and

THE UNIVERSITY OF KANSAS
LAWRENCE, KANSAS

November 2024

© Copyright 2024, **Kansas Department of Transportation**

PREFACE

The Kansas Department of Transportation's (KDOT) Kansas Transportation Research and New-Developments (K-TRAN) Research Program funded this research project. It is an ongoing, cooperative and comprehensive research program addressing transportation needs of the state of Kansas utilizing academic and research resources from KDOT, Kansas State University and the University of Kansas. Transportation professionals in KDOT and the universities jointly develop the projects included in the research program.

NOTICE

The authors and the state of Kansas do not endorse products or manufacturers. Trade and manufacturers names appear herein solely because they are considered essential to the object of this report.

This information is available in alternative accessible formats. To obtain an alternative format, contact the Office of Public Affairs, Kansas Department of Transportation, 700 SW Harrison, 2nd Floor – West Wing, Topeka, Kansas 66603-3745 or phone (785) 296-3585 (Voice) (TDD).

DISCLAIMER

The contents of this report reflect the views of the authors who are responsible for the facts and accuracy of the data presented herein. The contents do not necessarily reflect the views or the policies of the state of Kansas. This report does not constitute a standard, specification or regulation.

Abstract

Range anxiety is a significant contributor to consumer reticence when purchasing Electric Vehicles (EVs); thus, industry is pushing the range of EVs by enhancing lithium-ion battery chemistry. As a result, new commercial EVs readily achieve over 200 miles of range as found by the United States Environmental Protection Agency (EPA). However, this measured range by the EPA is often not the case when real-world conditions are encountered. The choice of testing indoors in idealized conditions (i.e., 77 ºF with the cabin conditioning system turned off) can belie the true range of EVs. This can be particularly problematic as government entities look to add charging stations nationwide. Any use of range that feeds into planning purposes must include on-road information such as wind (particularly important for the authors' home state of Kansas) and other facets like road grade and ambient temperature. Thus, this effort describes the simplest model that incorporates all important factors that impact the range of an EV. Calibration of the model to EPA tests found an average deviation of 0.45 and 0.57 miles for the highway and city ranges, respectively, over seven commercial EVs; hence, demonstrating good model accuracy. Subsequent predictions found significant losses based on the impact of road grade, wind, and vehicle speed over a Kansas interstate highway. In addition, up to 57.8% and 37.5% losses in range were found when simulating vehicles at 20 ºF and 95 ºF, respectively. Simulated aging of the vehicle battery pack due to cycling demonstrated range losses up to 53.1% at 100,000 miles. Model extensions to rain and snow illustrated corresponding losses based on the level of precipitation on the road. Finally, all model outcomes were translated into simple Excel spreadsheets that can be used in predicting the range of a generic EV over Kansas-centric roads.

Acknowledgements

We gratefully acknowledge the efforts of Allison Smith at the Kansas Department of Transportation for her help in improving the predictive nature of the model and her constant review of the material as our Project Monitor.

Table of Contents

List of Tables

List of Figures

Nomenclature

Variable	Description	Units
a	Parameter in distance determination	[-]
a_{aux}, b_{aux}, c_{aux}	Auxiliary power draw parameters	[W], [W s m^{-1}], [W s^2 m^{-2}]
a_{EPA}, b_{EPA}, c_{EPA}	EPA rolling resistance and drag coefficients	[N], [N s m^{-1}], [N s^2 m^{-2}]
A_f	Frontal area of vehicle	[m^2]
Ah	Battery pack capacity	[A h]
Ah^0	Initial capacity of battery pack	[A h]
a_{rr}, b_{rr}, c_{rr}	Rolling resistance parameters	[N], [N s m^{-1}], [N s^2 m^{-2}]
a_{rt}, b_{rt}, c_{rt}	Precipitation parameters for rolling resistance	[-], [m^{-1}], [s m^{-2}]
a_{YM}, b_{YM}, c_{YM}, d_{YM}, e_{YM}, f_{YM}	Energy consumption parameters for HVAC system on	[kWh mi^{-1}], [kWh mi^{-1} °F^{-1}], [kWh mi^{-1} °F^{-2}], [kWh mi^{-1} °F^{-3}], [kWh mi^{-1} °F^{-4}], [kWh mi^{-1} °F^{-5}]
c	Parameter in distance determination	[-]
C_D	Drag coefficient	[-]
c_m	Battery pack capacity multiplier	[-]
c_y	Battery pack cycles	[-]
d	Distance	[m]
D_{phase}	Distance of each phase of EPA test	[m]
E	Elevation	[m]
E_{aux}	Energy consumption per unit distance	[kWh mi^{-1}]
$ECdc_{cycle}$	Total energy consumption per unit distance	[W h m^{-1}]
$ECdc_{phase}$	Energy consumption per phase of EPA test	[W h m^{-1}]
Edc_{phase}	DC energy consumption per phase of EPA test	[W h]
F	Scaling factor on HVAC engaged models	[-]
F_D	Drag force	[N]
F_G	Gradation force	[N]
F_R	Rolling resistance force	[N]

F_T	Traction force	[N]
F_x	Acceleration or deceleration force	[N]
g	Standard gravity	[m s^{-2}]
GP	Maximum gradient of road	[deg]
i_0	Final drive gear ratio	[-]
i_g	Transmission gear ratio	[-]
I_{pack}	Pack amperage	[A]
I_{ref}	Reference amperage	[A]
I_t	Amperage of a single representative battery	[A]
K_{UDDS}	Scaling factor of UDDS cycle	[-]
K_{cycle}	Cycle scaling factor	[-]
K_{phase}	Phase scaling factor	[-]
lat	Latitude	[deg]
lon	Longitude of vehicle location	[deg]
m	Overall mass of vehicle	[kg]
n	Time-step	[-]
N	Motor speed	[rev min^{-1}]
n_{cycle}	Number of cycles for EPA test	[-]
N_{par}	Number of batteries in parallel	[-]
P_{aux}	Auxiliary power draw	[W]
P_b	Brake power	[W]
P_m	Motor power	[W]
P_r	Regenerative braking power	[W]
p_{ref}	Reference pressure	[kPa]
p_{tire}	Tire pressure	[kPa]
q_{dr}	Map driving direction	[deg]
q_{wind}	Wind direction	[deg]
R_{cycle}	Range of EV for cycle	[m]
r_d	Tire radius	[m]
R_{Earth}	Radius of Earth	[m]
SOC	State of Charge	[-]
t	Time	[s]

T_{amb}	Ambient temperature	[K]
T_{ref}	Reference temperature	[K]
t_{rt}	Thickness of rain or snow	[m]
T_t	Battery pack temperature	[K]
UBE	Total usable battery energy	[W h]
U_w	Wind speed in *x*-direction	[m s^{-1}]
V	Current vehicle velocity	[m s^{-1}]
$\bar{V}$	Average vehicle velocity	[m s^{-1}]
V_{cabin}	Cabin volume	[m^3]
V_{eff}	Effective vehicle velocity	[m s^{-1}]
V_{pack}	Current pack voltage	[VDC]
$\bar{V}_{pack}$	Average pack voltage over time-step	[VDC]
V_w	Wind speed in *y*-direction	[m s^{-1}]
V_{wind}	Wind speed	[m s^{-1}]
x	Parameter in bearing calculation	[-]
y	Parameter in bearing calculation	[-]
Z_{ref}	Reference weight	[N]

Greek Variables

Variable	Description	Units
α	Tire pressure exponent for rolling resistance	[-]
α_{aux}	Temperature exponential factor for HVAC system off	[-]
β	Weight exponent for rolling resistance	[-]
β_{br}	Bearing angle	[deg]
γ, χ, δ	Capacity offset parameters	[W], [-], [-]
ΔAh	Battery pack capacity change	[A h]
Δf	Difference in latitude between time-steps	[deg]
Δl	Difference in longitude between time-steps	[deg]
Δt	Time-step	[s]
ΔWh	Change in battery pack energy	[W h]
h_m	Motor efficiency	[-]
h_t	Driveline efficiency	[-]
φ	Yaw angle of the vehicle	[rad]
ϑ	Angle of wind relative to direction of motion	[rad]
θ	Roadway slope	[deg]
ρ	Density of air	[kg m^{-3}]
μ_r	Rolling resistance coefficient	[-]
τ_b	Brake torque	[N m]
τ_w	Wheel torque	[N m]

Acronyms

AAA	American Automobile Association
CSC	Constant Speed Cycle
E	East
EPA	Environmental Protection Agency
EV	Electric Vehicle
GPS	Global Positioning System
HVAC	Heating, Ventilation, and Air Conditioning
HWFET	Highway Fuel Economy Test
MCT	Multi-Cycle Test
MPG_e	Miles Per Gallon Equivalent
N	North
NCA	Nickel Cobalt Aluminum Oxide
NCM_{333}	$LiNi_{1/3}Co_{1/3}Mn_{1/3}O_2$
NCM_{523}	$LiNi_{0.5}Co_{0.2}Mn_{0.3}O_2$
NCM_{622}	$LiNi_{0.6}Co_{0.2}Mn_{0.2}O_2$
S	South
SAE	Society of Automotive Engineers
UDDS	Urban Dynamometer Driving Schedule
US06	Supplemental Federal Test Procedure
W	West

Chapter 1: Introduction

While battery technology has improved significantly over the last decade, range anxiety is still a primary consideration for consumers when contemplating the purchase of an Electric Vehicle (EV) (Pevec et al., 2020). A recent survey by Autolist found that EV range tops the consumers' list of priorities (Autolist Analytics Team, 2021) with one of their earlier surveys indicating that the majority of respondents considered 300 miles of range to be sufficient (Voelcker, 2017). While most commercially available EVs are now able to achieve greater than 200 miles range, with the Tesla Model 3 sporting a 353 mile range according to the Environmental Protection Agency (EPA), the actual on-road range of EVs is based on a variety of factors (e.g., weather, weight, road grade, and cabin conditioning) and can be significantly different than the ideal conditions employed by the EPA during the Society of Automotive Engineers (SAE) J1634 test (77 ºF using a chassis dynamometer with the cabin conditioning system turned off) (SAE J1634, 2017). Thus, the varying range experienced by EV drivers can be problematic when designing a charging infrastructure to handle their range anxiety while considering the travel route and weather conditions (Ahn & Yeo, 2015). This is especially true in Kansas when considering the wide range of conditions encountered by Kansas drivers, in addition to being the second windiest state in the union (Samenow, 2016) while also encountering all four seasons with potentially significant rainfall and snow (Lin et al., 2017).

Additional factors that can cause EPA vehicle range tests to misrepresent real-world driving include greater passenger and cargo loads that will increase energy consumption (Weiss et al., 2020). Furthermore, EPA tests also do not consider road grade that can result in increased or decreased range depending on the slope gradient (Liu et al., 2017). Al-Wreikat et al. (2021) found that a 3% road grade could increase energy consumption by 50% or more. However, a downward grade can be beneficial, as gravity reduces the traction force required to maintain a certain speed, while also potentially recharging the battery pack through regenerative braking. This ability to recharge the battery pack while braking is one reason why EVs typically demonstrate a greater range in the city than on the highway, counter to more traditional internal combustion engine vehicles.

Other significant impacts on EV range are the rolling resistance and aerodynamic drag. Under low speeds when road grade is negligible, rolling resistance and drag make up the total forces acting on the vehicle that must be overcome (Pavlat & Diller, 1993). While the EPA test does include a combined factor for both of these components, the impact of wind speed and direction on drag is not considered (Yi & Bauer, 2017; Sarrafan et al., 2018). In addition, the increased rolling resistance due to underinflated tires can lead to EV range losses of a few percent (Tang et al., 2020). Weather can also play a substantial role in rolling resistance as rain can increase this resistance by up to 10% (Tannahill et al., 2016). Analogously, snow can increase rolling resistance by 6-9% depending on if the snow is old or freshly fallen (Laurikko et al., 2012). Thus, researchers should incorporate these effects into their models (Sarrafan et al., 2017).

Weather further contributes to decreases in EV range when ambient temperature is considered. This is primarily due to energy being used for cabin conditioning and thermal conditioning of the battery pack. Higher temperatures typically accelerate the fading of the battery or decrease the efficiency of the motor, as Hao et al. (2020) found that electrical consumption increased 126.3 Btu/mi with every 9 °F over 82.4 °F (2.3 kWh/100 km with every 5 ºC over 28 ºC.) Furthermore, Samadani et al. (2014) showed that the air conditioning system can reduce range by 14%, 22%, and 20% for the HWFET, UDDS, and US06 standard drive cycles, respectively, while also increasing battery degradation. Here, the impact of higher temperatures on range is not as significant as the influence of colder temperatures. Without a heater in use, the average range from different driving cycles will decrease up to 20-30% in cold weather (Laurikko et al., 2012). Conversely, when the full cabin heating is in use, the range may be reduced by as much as 60% (Horrein et al., 2017; Szumska & Jurecki, 2021).

Apart from mechanical or electrical losses, the driving method and behavior of the driver can influence the range of an EV. Faster accelerations have been found to increase the energy intensity by 4% over the slowest acceleration simulated for a 1000 kg EV (Mruzek et al., 2016). In general, aggressive driving increases energy consumption between 16% and 43% when compared to passive driving (Laurikko et al., 2012; Al-Wreikat et al., 2021). This is caused by an inefficient use of the vehicle's acceleration and braking mechanisms (Laurikko et al., 2012).

Given this wide variance in energy usage and corresponding EV range, it is important for local municipalities and state agencies to have a simulation tool that can estimate the range of commercial EVs in their local environment. This can then be used to facilitate the process planning of an effective charging station infrastructure. While extensive models exist for motors, batteries, air conditioning, and other aspects of EVs, this effort endeavors to generate a simple overarching model that includes all necessary variables to estimate the range of EVs on local roads based on the time of year. Overall, six commercial EVs were calibrated to their EPA stated range and parametric studies were completed to understand the different aspects that influence range over the following Kansas roads: I-70, I-35, US-54, and I-135. In addition, the model is employed to predict the range of an EV that is not commercially available yet as an exercise to understand how the real range of the vehicle in Kansas compares to the EPA stated range. The subsequent sections of this work include a description of the model developed, followed by a summary of the resulting parametric studies.

Chapter 2: Modeling

A previous effort by one of the authors included the estimation of battery electric heavy-duty tractor trailers using a model based on the conservation of momentum (i.e., Newton's second law of motion) (Depcik et al., 2019). This work utilized a similar model including additions to handle wind direction based on travel direction and electrical power requirements. Overall, the resultant acceleration or deceleration force (F_x) was determined from the tractive (F_T), aerodynamic drag (F_D), rolling resistance (F_R), and gradation forces (F_G) as follows:

$$\boldsymbol{F_x = F_\mathrm{T} - F_\mathrm{D} - F_\mathrm{R} - F_\mathrm{G}}$$

Equation 2.1

However, when simulating the SAE J1634 test to determine the highway and city mileage range (SAE J1634, 2017), the drag and rolling resistance forces are combined and accounted for by a chassis dynamometer via a polynomial function (Kadijk & Ligterink, 2012) with the coefficients published online by the EPA (U.S. Environmental Protection Agency, n.d.):

$$\boldsymbol{F_\mathrm{D} + F_\mathrm{R} = a_{EPA} + b_{EPA}\bar{V} + c_{EPA}\bar{V}^2}$$

Equation 2.2

Where $\bar{V}$ is the average velocity of the vehicle between two successive input data points (velocity is a specified input parameter) represented by the superscript n:

$$\boldsymbol{\bar{V} = \frac{V^{n+1} + V^n}{2}}$$

Equation 2.3

Otherwise, the forces are independent, and the drag force is represented as:

$$\boldsymbol{F_\mathrm{D} = \frac{1}{2}\rho A_f C_D (V_{eff} cos\varphi)^2}$$

Equation 2.4

Where ρ is the density of the air (determined using the ideal gas law) and C_D is the coefficient of drag. The frontal area of the vehicle (A_f) was determined using a computer program that digitized the vehicle front view that was calibrated to a reference value for the overall width of the vehicle (SketchAndCalc, n.d.).

2.1 Wind Speed and Direction

The effective vehicle velocity (V_{eff}) is a function of the yaw angle of the vehicle (φ) and the wind speed (V_{wind}):

$$\boldsymbol{V_{eff}cos\varphi = \bar{V} - V_{wind}cos\vartheta}$$

Equation 2.5

While yaw can be important, it was neglected here because of the difficulty involved in calculating it accurately over the length of the route. To account for the angle of wind relative to the direction of motion (ϑ), latitude (lat) and longitude (lon) coordinates were employed from Global Positioning System (GPS) data that can also provide elevation (E) data. Between two successive GPS data points, the change in distance (d) was determined as:

$$\boldsymbol{d^{n+1} - d^{n} = R_{Earth}c}$$

Equation 2.6

Where R_{Earth} is Earth's radius ($2.0926 \cdot 10^7$ ft) ($6378.1 \cdot 10^3$ m) (Prša et al., 2016) and c is determined by (Sinnott, 1984):

$$\boldsymbol{c = 2 \cdot atan2\left(\sqrt{a}, \sqrt{1-a}\right)}$$

Equation 2.7

$$\boldsymbol{a = sin^2\left(\frac{\Delta f}{2}\right) + cos(lat^n)cos(lat^{n+1})sin^2\left(\frac{\Delta l}{2}\right)}$$

Equation 2.8

$$\boldsymbol{\Delta f = lat^{n+1} - lat^{n}}$$

Equation 2.9

$$\boldsymbol{\Delta l = lon^{n+1} - lon^{n}}$$

Equation 2.10

The bearing angle of the vehicle (β_{br}) was also obtained from GPS data and altered to correspond to a 360° North (N)-South (S)/East (E)-West (W) map driving direction (q_{dr}):

$$\boldsymbol{q_{dr} = \begin{cases} 450 - \beta_{br}, & x < 0 \; and \; y > 0 \\ 90 - \beta_{br}, & else \end{cases}}$$

Equation 2.11

$$\boldsymbol{\beta_{br} = atan2\,(y, x)}$$

Equation 2.12

The output is an angle from 0 to π or 0 to – π. Thus, q_{dr} was obtained through a piecewise function that accounts for the quadrant of the resulting vector and converts the computed angle from the "unit circle" frame to the N-S/E-W frame. The x and y components were determined, respectively, as:

$$\boldsymbol{x = cos(lat^{n+1})sin(\Delta l)}$$

Equation 2.13

$$\boldsymbol{y = cos(lat^{n})sin(lat^{n+1}) - sin(lat^{n})cos(lat^{n+1})cos(\Delta l)}$$

Equation 2.14

The angle and speed of the wind were determined similarly from their corresponding x- and y-directions, U_w and V_w, respectively:

$$\boldsymbol{q_{wind} = \begin{cases} 450 - \text{atan2}(V_w, U_w), & U_w < 0 \; and \; V_w > 0 \\ 90 - \text{atan2}(V_w, U_w), & else \end{cases}}$$

Equation 2.15

$$\boldsymbol{V_{wind} = \sqrt{{U_w}^2 + {V_w}^2}}$$

Equation 2.16

This was then combined with the driving direction to find the angle of wind relative to the direction of motion:

$$\boldsymbol{\vartheta = q_{wind} - q_{dr}}$$

Equation 2.17

Twenty years (2000-2020) of wind speed information delineated by month for the state of Kansas (the authors' home state) was captured from National Oceanic and Atmospheric Administration data (National Centers for Environmental Information, 2021).

2.2 Rolling Resistance

The rolling resistance force in Equation 2.1 can be expressed in a simplistic manner using a singular rolling resistance coefficient (μ_r) employing the overall mass of the vehicle (m) times the acceleration due to gravity (g):

$$\boldsymbol{F_R = \mu_r mg}$$

Equation 2.18

A more complex expression that is a function of tire pressure (p_{tire}) and vehicle velocity, also, is (Hausmann & Depcik, 2014):

$$F_R = \left(\frac{p_{tire}}{p_{ref}}\right)^{\alpha} \left(\frac{mg}{Z_{ref}}\right)^{\beta} (a_{rr} + b_{rr}\bar{V} + c_{rr}\bar{V}^2)$$

Equation 2.19

Including reference parameters (p_{ref} = 1 kPa, Z_{ref} = 1 N). Since the model was initially calibrated to match EPA data (discussed in Section 2.7) utilizing chassis dynamometer information (Equation 2.2), this allowed for calibration of this rolling resistance function to determine the constants (a_{rr}, b_{rr}, and c_{rr}). For the parameters α and β, values by Grover were utilized for a P195/70R14 tire: -0.345 and 0.929, respectively (Grover, 1998). Ideally, these values should be found for each tire utilized by the EVs; however, this information was not available. Therefore, simulating different tire pressures and vehicle weights other than the EPA test values will incur some error. However, the respective trends will be informative and provide a better representation rather than the use of a singular rolling resistance coefficient. One oversight not considered with this model is that tire pressure will change based on ambient temperatures (e.g., 1.566-2.031 psi/18 °F [0.108-0.140 bar/10° C][Fechtner et al., 2015]); however, this could be added in the future.

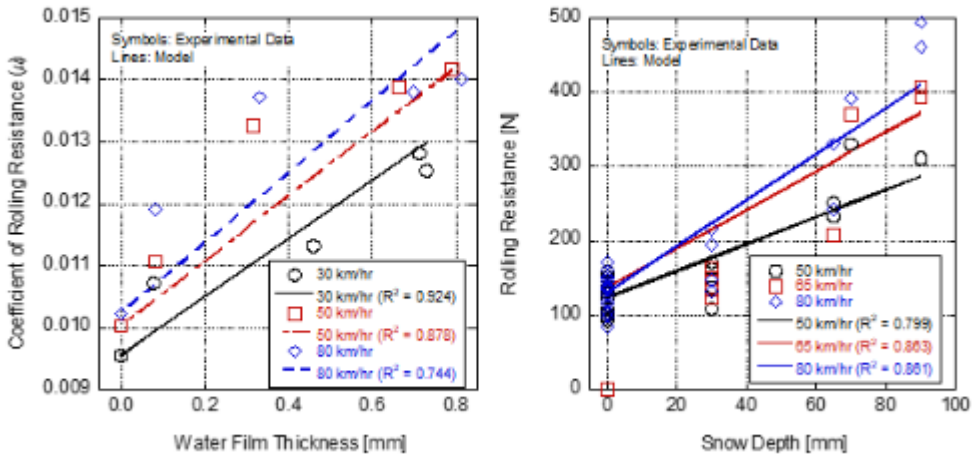

Figure 2.1: Comparison of Rolling Resistance Model Predictions and Experimental Data for Rain (Left) and Snow (Right)

To account for inclement weather conditions, rolling resistance coefficients (μ_r) as a function of water film thickness (i.e., rain) for a standard reference test tire (Ejsmont et al., 2015) and rolling resistance forces (F_R) based on snow thickness (Kihlgren, 1977) were found as shown in Figure 2.1. Using the available weights and tire pressures provided in these references, the values of the constants for Equation 2.19 without rain or snow were first found using the MATLAB *fmincon* function while minimizing the difference between the calculated μ_r or F_R based on the corresponding data:

Rain: a_{rr} = 2.134E-02 lbf, b_{rr} = 4.653E-03 lbm s^{-1}, and c_{rr} = -3.437E-05 lbm ft^{-1}
Snow: a_{rr} = -2.837E-02 lbf, b_{rr} = 1.009E-01 lbm s^{-1}, and c_{rr} = -8.178E-04 lbm ft^{-1}

Subsequently, a revised rolling resistance force model was generated to account for the respective thickness of the rain or snow (t_{rt}), respectively:

$$\boldsymbol{F_R = \left(\frac{p_{tire}}{p_{ref}}\right)^{\alpha}\left(\frac{mg}{Z_{ref}}\right)^{\beta}(a_{rr} + b_{rr}\bar{V} + c_{rr}\bar{V}^2)(a_{rt} + b_{rt}t_{rt} + c_{rt}\bar{V}t_{rt})}$$

Equation 2.20

Given the respective scatter of the data, a linear fit was initially chosen as higher order fits caused the rolling resistance to decrease at the largest water film level, which is erroneous. Since the data also indicates a velocity dependency, the last term in the added model components includes its influence. This model was then calibrated using the MATLAB *fmincon* function to minimize the difference between the calculated values and experimental data with the following results:

Rain: a_{rt} = 1, b_{rt} = 1.382E+02 ft^{-1}, c_{rt} = 4.349E-01 s·ft^{-2}
Snow: a_{rt} = 1; b_{rt} = -1.246E-01 ft^{-1}, c_{rt} = 1.004E-01 s·ft^{-2}

Overall, the results in Figure 2.1 demonstrate an acceptable fit (R^2 between 0.744 and 0.924).

2.3 Gradation and Acceleration/Deceleration Forces

The gradation force in Equation 2.1 involves the current slope of the roadway (θ):

$$\boldsymbol{F_G = mgsin\theta}$$

Equation 2.21

Determined using the elevation change over the distance travelled:

$$\boldsymbol{\theta = \tan^{-1}\left(\frac{E^{n+1} - E^{n}}{d^{n+1} - d^{n}}\right)}$$

Equation 2.22

Considering highways are regulated to have a maximum gradient (*GP*) of 7% (American Association of State Highway and Transportation Officials, 2001), a conditional statement was implemented to limit the grade experienced along the route to a maximum of 7% resulting in a slope angle of about 4 degrees:

$$\boldsymbol{\theta = \tan^{-1}(GP/100)}$$

Equation 2.23

The net vehicle force (i.e., acceleration or deceleration of the vehicle) in the travelled direction is expressed as:

$$\boldsymbol{F_x = m\frac{dV}{dt}}$$

Equation 2.24

Using a Euler Explicit differentiation, the velocity derivative can be simplified:

$$\boldsymbol{\frac{dV}{dt} = \frac{V^{n+1} - V^{n}}{\Delta t}}$$

Equation 2.25

The time-step in Equation 2.25 is calculated using the change in distance divided by the average vehicle speed:

$$\boldsymbol{\Delta t = \frac{d^{n+1} - d^{n}}{\bar{V}}}$$

Equation 2.26

2.4 Torques, Engine Speed, and Power

At each time-step, the tractive force was calculated using Equation 2.1 allowing for the determination of the resulting wheel (τ_w) and brake torques (τ_b), respectively:

$$\boldsymbol{\tau_w = F_T \cdot r_d}$$

Equation 2.27

$$\boldsymbol{\tau_b = \frac{\tau_w}{i_0 i_g h_t}}$$

Equation 2.28

Where r_d, i_0, i_g, and h_t are the tire radius, the final drive gear ratio, transmission gear ratio, and driveline efficiency, respectively. The influence of driveline efficiency was incorporated through an auxiliary power draw (discussed in the next section); hence, for this expression it was given a value of one.

Next, the motor speed (N) was calculated by using the average velocity:

$$\boldsymbol{N = \frac{\bar{V} i_0 i_g}{2\pi r_d}}$$

Equation 2.29

In combination with the brake torque, this value was utilized to determine the brake power (P_b) that was employed to evaluate motor power (P_m) using the efficiency of the motor (h_m).

$$\boldsymbol{P_b = 2\pi \tau_b N}$$

Equation 2.30

$$\boldsymbol{P_m = \frac{P_b}{h_m}}$$

Equation 2.31

With a three-dimensional motor map implemented based on motor torque and speed. For simplicity, the map for regenerative braking was assumed to be the same as the motor map, although they will differ slightly. In addition, regenerative braking power (P_r) was determined slightly differently (i.e., power used by the motor during acceleration should be more than the braking power), whereas the power recovered by the motor during braking/regeneration should be less than the braking power.

$$\boldsymbol{P_r = h_m P_b}$$

Equation 2.32

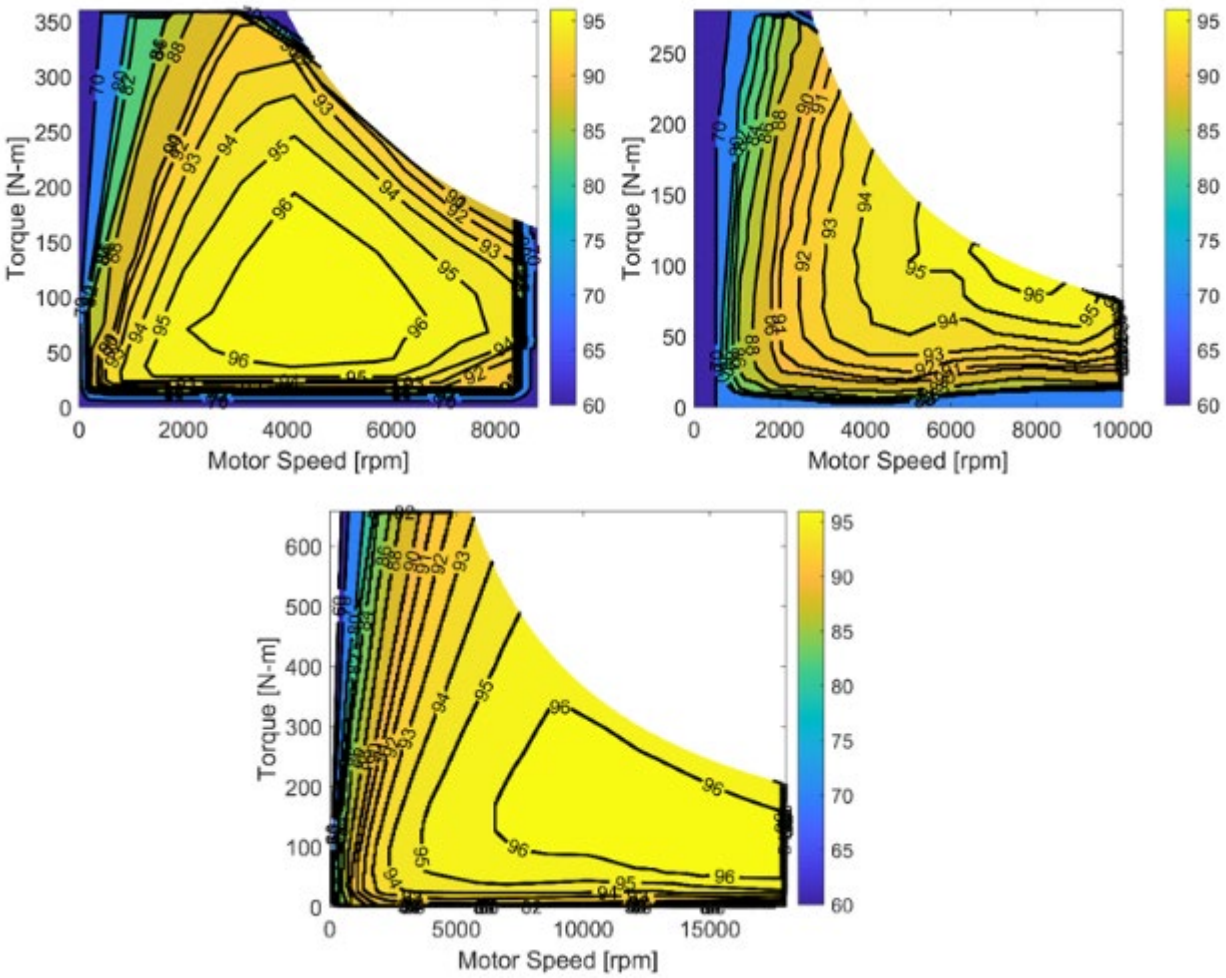

Figure 2.2: Motor Efficiency Maps for (Top Left) Permanent Magnet Synchronous Motor A, (Top Right) Permanent Magnet Synchronous Motor B, and (Bottom) Induction Motor

Three motors maps were found to account for two different permanent magnet synchronous motors (A – [Momen et al., 2016] and B – [Burress, 2013]) and an induction motor (Staton & Goss, 2017) as provided in Figure 2.2. Unfortunately, the need to digitize these maps required estimating a few values near the origin and out of the maximum power area. In addition, if it is found maximum torque and maximum speed of a vehicle's motor were greater than the corresponding map chosen, then the map was scaled by these respective parameters to ensure that it captures the entire operating range. As a result, there is some error in this estimation of motor (and regeneration) efficiency, and it would be preferred to use the exact motor map data. Another simulation approach could be to employ the model of Larsson (2014) that estimates motor efficiency as a function of torque and rotational speed and then calibrate the constants to available

map data. This would provide quicker simulation results and potentially handle data near zero torque and zero motor speed more effectively.

Subsequently, the amperage draws (I_{pack}) from the battery pack was found using its voltage from a look-up table based on the current State of Charge (SOC) under different discharge currents (indicated in Section 2.6).

$$\boldsymbol{I_{pack} = \frac{P_m + P_{aux}}{\bar{V}_{pack}}}$$

Equation 3.33

Where the average voltage of the pack over the time-step was used in an iterative procedure, i.e., V_{pack}^{n} was known and a new value (V_{pack}^{n+1}) was found based on an updated SOC^{n+1}. For this equation, the P_{aux} parameter includes all auxiliary system draws as discussed in the next section.

2.5 Auxiliary Power

With respect to driveline efficiency, there are losses resulting from the conversion of battery energy into useful torque. Other systems, such as the inverter, lights, windows, etc., also consume energy during operation and must be considered when estimating the range of an EV. Evtimov et al. (2017) characterized these specific energy consumptions by polynomials up to the sixth order as a function of vehicle speed. In the scenario when heating or air conditioning is not required, this power draw was estimated using a second-order polynomial while additionally including a temperature factor:

$$\boldsymbol{P_{aux,HVAC_{off}} = (a_{aux} + b_{aux}\bar{V} + c_{aux}\bar{V}^2)\left(1 + \left|\frac{T_{amb} - 298.15K}{298.15K}\right|\right)^{\alpha_{aux}}}$$

Equation 2.34

The respectively simplistic temperature factor expression was based on findings from the American Automobile Association (AAA) that found small reductions in driving range of commercial EVs in hot and cold ambient conditions when the heating, ventilation, or air conditioning (HVAC) system is not engaged (American Automobile Association, 2019). Here, three parameters (a_{aux}, b_{aux}, and c_{aux}) are used as calibration for the model to match the SAE J1634 test for the EPA City and Highway range values (discussed in Section 2.7) at 77 °F (25 °C)

with the HVAC system off (U.S. Department of Energy & U.S. Environmental Protection Agency, 2021). The temperature factor (α_{aux}) considers the relative losses found during testing by AAA at 20 °F and 95 °F from their standard data state of 75 °F.

When the HVAC system is engaged, Yuksel and Michalek (2015) generated a polynomial fit for this energy consumption per unit distance (E_{aux}) in (kWh·mi^{-1}) with the ambient temperature in (°F):

$$\boldsymbol{E_{aux} = a_{YM} + b_{YM}T_{amb} + c_{YM}T_{amb}^2 + d_{YM}T_{amb}^3 + e_{YM}T_{amb}^4 + f_{YM}T_{amb}^5}$$

Equation 2.35

This model includes the effects of cabin conditioning and battery efficiency as a function of ambient conditions while isolating the temperature effect from location-specific influences (i.e., driving conditions). Similar to a prior effort (Depcik et al., 2019), E_{aux} was multiplied by the velocity to obtain the power draw from the battery pack due to the HVAC system operating. However, analogous to Equation 2.34, a second order polynomial was used for the velocity component:

$$\boldsymbol{P_{aux,HVAC_{on}} = (a_{aux} + b_{aux}\overline{V} + c_{aux}\overline{V}^2)E_{aux}}$$

Equation 2.36

All constants in Equation 2.35 and 2.36 were calibrated (again using the MATLAB *fmincon* function to minimize differences between experimental data and the model) to account for the losses found during the AAA tests at 20 °F and 95 °F when the HVAC system was engaged (again away from their standard state of 75 °F). Note that temperature in Equation 2.35 was left in degrees Fahrenheit to be consistent with Yuksel and Michalek's (2015) formulation and the use of kelvin provided less model fidelity (i.e., using kelvin with a sixth-order temperature term causes the value of E_{aux} to change dramatically over a 1 kelvin temperature difference).

2.6 Batteries

To calculate capacity losses (or gains) of the battery pack (ΔAh) as power is required (or regenerated), the Hausmann and Depcik model was implemented where the constants γ, χ, and δ describe the capacity offset of the battery (Hausmann & Depcik, 2013; O'Malley et al., 2018):

$$\Delta \boldsymbol{Ah} = \boldsymbol{\gamma}\left(\frac{\boldsymbol{I_t}}{\boldsymbol{I_{ref}}}\right)^{\chi}\left(\frac{\boldsymbol{T_{ref}}}{\boldsymbol{T_t}}\right)^{\boldsymbol{\delta}}\Delta \boldsymbol{t}$$

Equation 2.37

Both the reference temperature (T_{ref}) and reference amperage draw (I_{ref}) are 298 K and 1 A, respectively. Based on the specific chemistry of the battery for each EV, representative singular battery voltage versus depth of discharge data were found (Figure 2.3 through Figure 2.6) and the simulation assumed that all batteries act similarly. Therefore, the pack amperage draw was reduced by the number of batteries in parallel (N_{par}) to find the amperage required by a singular battery (I_t):

$$\boldsymbol{I_t} = \frac{\boldsymbol{I_{pack}}}{\boldsymbol{N_{par}}}$$

Equation 2.38

Unfortunately, for a few chemistries, temperature specific data were not found; hence, the δ parameter was set to zero. Overall, data for $LiNi_{1/3}Co_{1/3}Mn_{1/3}O_2$ (NCM_{333}) (Samsung, 2015), $LiNi_{0.5}Co_{0.2}Mn_{0.3}O_2$ (NCM_{523}) (Kwon et al., 2018), $LiNi_{0.6}Co_{0.2}Mn_{0.2}O_2$ (NCM_{622}) (Kwon et al., 2018), and two nickel cobalt aluminum oxide (NCA_1 and NCA_2) (Panasonic, 2012; ZeroAir Reviews, 2018) batteries were found. For simulation purposes, the temperature of the battery (T_t) was set to the reference temperature since it is assumed that the battery management system endeavors to maintain the chemistry at its ideal level. Calibration of the capacity offset parameters is described in O'Malley et al. (2018).

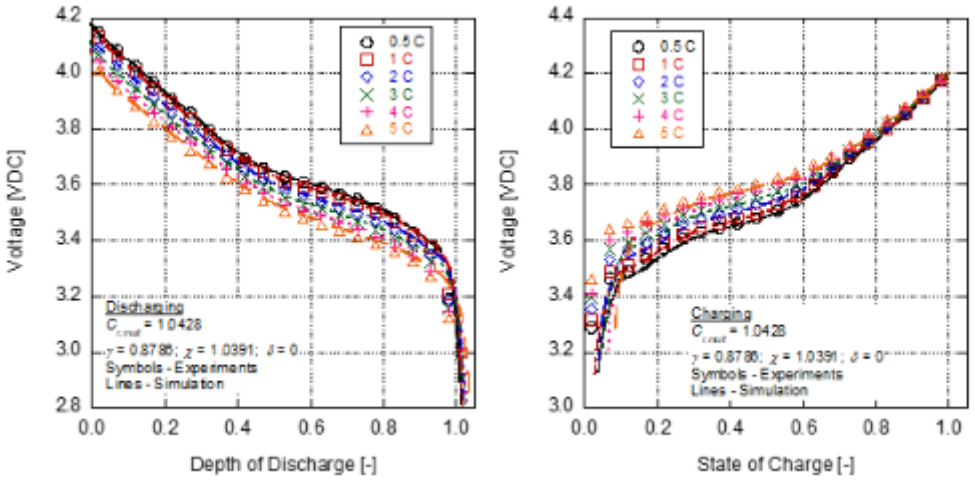

Figure 2.3: Experimental Data and Model Results of a Representative NCM_{622} Battery

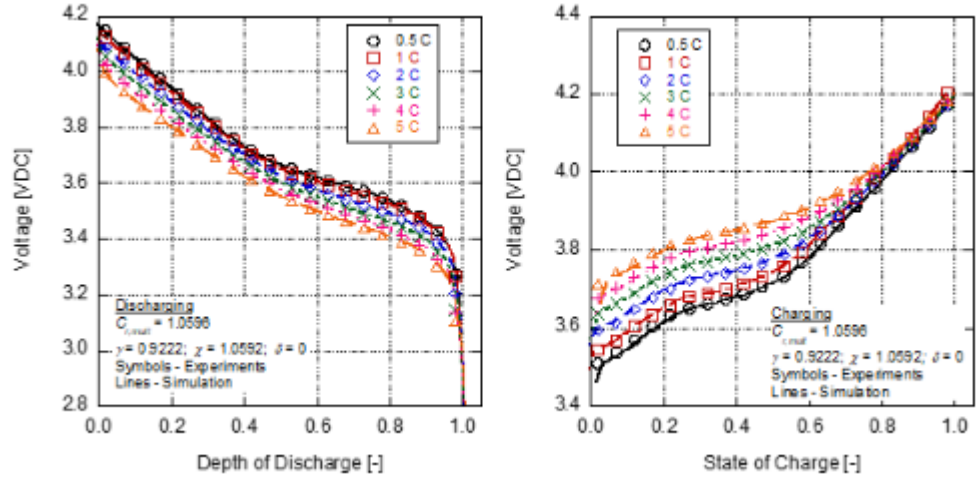

Figure 2.4: Experimental Data and Model Results of a Representative NCM_{523} Battery

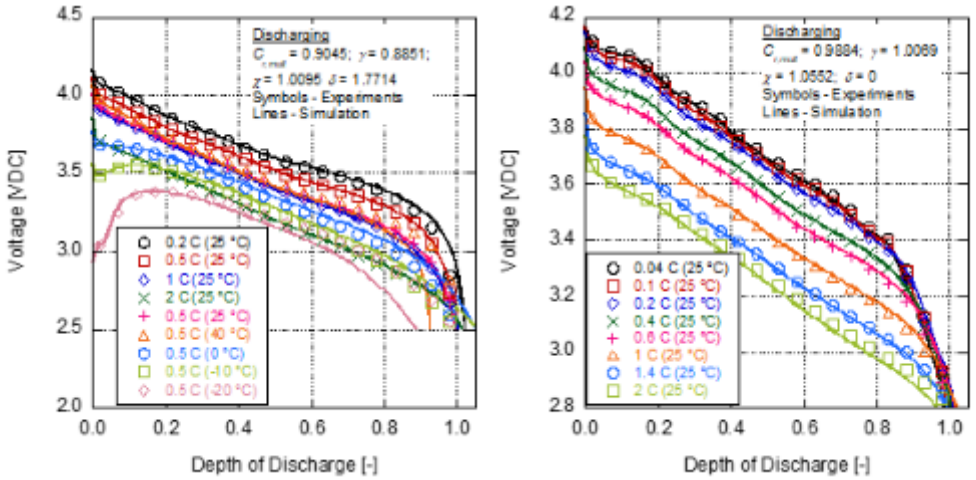

Figure 2.5: Experimental Data and Model Results of Representative NCA Batteries (NCA_1 – Left, NCA_2 – Right)

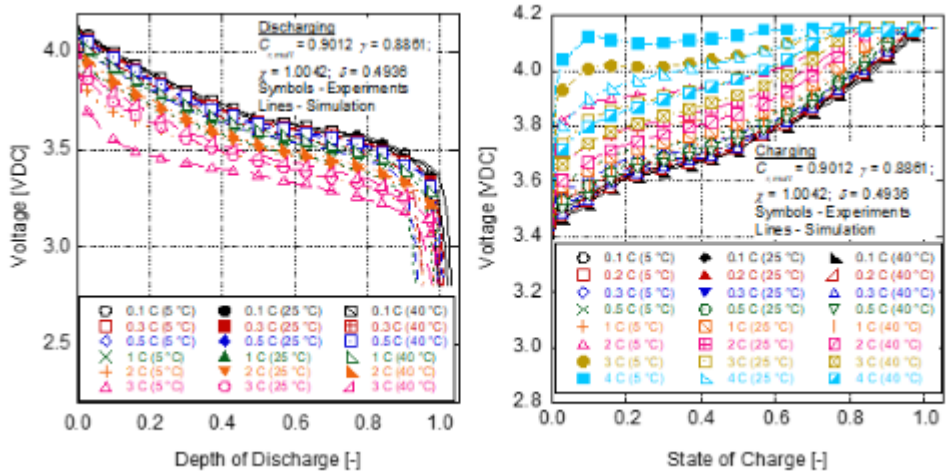

Figure 2.6: Experimental Data and Model Results of a Representative NCM_{333} Battery

Starting with an initial battery pack capacity (Ah^0), it loses capacity according to the following equation, with Ah^n the capacity of the current time step and Ah^{n+1} the capacity of the next step:

$$\boldsymbol{Ah^{n+1} = Ah^n - \Delta Ah}$$

Equation 2.39

Then, the SOC of the batteries can be found from the initial capacity:

$$\boldsymbol{SOC^{n+1} = \frac{Ah^{n+1}}{Ah^0}}$$

Equation 2.40

Overall, by using the time step over the simulation and the known power draws, the energy required by the battery pack during this time step can be calculated and expressed in watt-hours (Wh):

$$\Delta \boldsymbol{Wh} = \Delta \boldsymbol{t}(\boldsymbol{P_m} + \boldsymbol{P_{aux}})$$

Equation 2.41

It has been shown that as EVs age, their range also decreases (Saxena et al., 2015). To account for this facet, polynomial curve-fits were incorporated that estimate the percentage of capacity remaining (c_m) in the battery pack after several cycles (c_y) ($R^2 \sim 0.996$) at 77 °F (25 °C):

$$\textbf{NCM}_{622}\textbf{: } \boldsymbol{c_m = 100 - 7.525 \times 10^{-3} c_y - 1.784 \times 10^{-5} {c_y}^2 + 9.003 \times 10^{-9} {c_y}^3 - 1.507 \times 10^{-12} {c_y}^4}$$

Equation 2.42

$$\textbf{NCM}_{523}\textbf{: } \boldsymbol{c_m = 100 + 7.313 \times 10^{-3} c_y - 1.764 \times 10^{-5} {c_y}^2 + 9.312 \times 10^{-9} {c_y}^3 - 1.559 \times 10^{-12} {c_y}^4}$$

Equation 2.43

$$\textbf{NCM}_{622}\textbf{: } \boldsymbol{c_m = 100 - 7.525 \times 10^{-3} c_y - 1.784 \times 10^{-5} {c_y}^2 + 9.003 \times 10^{-9} {c_y}^3 - 1.507 \times 10^{-12} {c_y}^4}$$

Equation 2.44

$$\textbf{NCM}_{333}\textbf{: } \boldsymbol{c_m = 100 - 3.269 \times 10^{-3} c_y - 3.223 \times 10^{-6} {c_y}^2 + 1.878 \times 10^{-9} {c_y}^3 - 3.380 \times 10^{-13} {c_y}^4}$$

Equation 2.45

This percentage capacity remaining was then multiplied by the initial capacity (Ah^0) to determine the pack capacity as a function of an initial starting cycle. The coefficients were determined by matching the polynomials to experimental data in Figure 2.7 (NCM_{622} and NCM_{523} [Kwon et al., 2018], NCA [Panasonic, 2012], and NCM_{333} [Samsung, 2015]). Note that the NCA data was linearly extrapolated from the last two data points until 3000 cycles and the model fit these data for completeness.

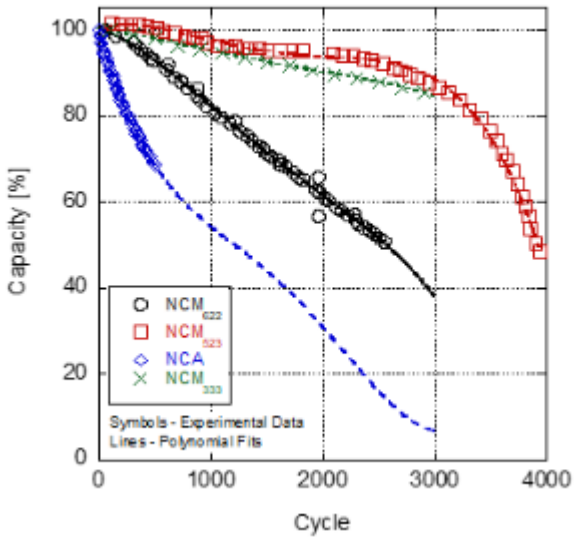

Figure 2.7: Loss in Capacity of Representative Batteries Based on Cycle Life

2.7 SAE J1634 Calculations and Considerations

The initial calibration of the model was accomplished according to the EPA data determined from the SAE J1634 standard (SAE J1634, 2017). In this standard, the equations needed to find vehicle city and highway ranges are provided as part of a Multi-Cycle Test (MCT) procedure. The general form for the range of a given cycle type (R_{cycle}) is as follows:

$$\boldsymbol{R_{cycle} = \frac{UBE}{ECdc_{cycle}}}$$

Equation 2.46

Where the total usable battery energy from the entire test (UBE) in W-h (i.e., sum of Equation 2.41 over the entire test) is divided by the total energy consumption per unit distance ($ECdc_{cycle}$) of a given cycle type (i.e., highway or city: W·h·m^{-1}). To find $ECdc_{cycle}$, the phase scaling factor (K_{phase_i}) is used in conjunction with the energy consumption per unit distance of a given phase ($ECdc_{phase_i}$):

$$\boldsymbol{ECdc_{cycle} = \sum\left(K_{phase_i} \cdot ECdc_{phase_i}\right)}$$

Equation 2.47

Where $ECdc_{phase_i}$ is found using the DC energy consumption (Edc_{phase_i}) and distance traveled of a given phase (D_{phase_i}):

$$\boldsymbol{ECdc_{phase_i} = \frac{Edc_{phase_i}}{D_{phase_i}}}$$

Equation 2.48

Additionally, K_{phase_i} is found for each phase of the test using the total number of phases of certain cycle ($n_{UDDS} = 4, n_{HWFET} = 2$):

$$\boldsymbol{K_{cycle_i} = \frac{1}{n_{cycle}}}$$

Equation 2.49

K_{phase_i} is equal to K_{cycle_i} for both phases of the HWFET (highway) cycle, but the UDDS (city) cycle requires an additional consideration. As a result of cold start regenerative braking limitations during the first phase of the UDDS cycle that occurs during the MCT test, there is overall increased energy consumption for the UDDS cycle. To counter this effect, an equivalent phase scaling factor ($K_{UDDS_{ie}}$) is used for each UDDS phase:

$$\boldsymbol{K_{UDDS_{1e}} = \frac{Edc_{UDDS_1}}{UBE}}$$

Equation 2.50

$$\boldsymbol{K_{UDDS_{2e}} = K_{UDDS_{3e}} = K_{UDDS_{4e}} = \frac{1 - K_{UDDS_{1e}}}{3}}$$

Equation 2.51

Two further considerations are needed regarding the SAE J1634 standard:

1. Vehicle must be aged at least 1000 miles, and
2. The Constant Speed Cycle (CSC) at the end of the MCT must be 20% or less of the total driving distance.

Regarding aging, it states that battery aging may be performed either with the vehicle (Durability Driving Schedules, 2011) or by using an equivalent bench test procedure (Idaho National Engineering Laboratory, 1996). Since it was not readily apparent how to translate the bench test procedure to vehicle miles, the methodology to age the vehicle using the durability driving schedule (UDDS) was employed (Durability Driving Schedules, 2011). In essence, the UDDS cycle was simulated for 1000 miles to determine the respective number of cycles (c_y) the battery pack underwent. Then, the capacity remaining polynomials in Section 4.6 were used to determine the respective value of c_m to be applied to the pack prior to simulating the SAE J1634 standard.

To properly model this driving cycle, values for maximum acceleration, normal acceleration, light acceleration, normal deceleration, and light deceleration had to be found from the literature. Taking the average value from various sources, 10.4 ft/s^2 and 3.31 ft/s^2 were obtained for maximum acceleration and normal acceleration, respectively (Proctor et al., 1995; Kleeman, 1998; Bokare & Maurya, 2017). As for light acceleration, a rate of 1.66 ft/s^2 corresponds to half of the normal acceleration value and falls within the low to medium range of acceleration seen in the UDDS drive cycle. For normal deceleration, an average of 8.30 ft/s^2 was found when stopping from a maximum speed ranging from 36.5 to 82 ft/s (Bennett & Dunn, 1995; Akçelik & Besley, 2001; Wang et al., 2005; Maurya & Bokare, 2012; Bokare & Maurya, 2017). Average deceleration from maximum speeds ranging from 82.9 to 91.1 ft/s was significantly less in magnitude, at an average of 3.953 ft/s^2 (Maurya & Bokare, 2012), and thus, was used for modeling light deceleration.

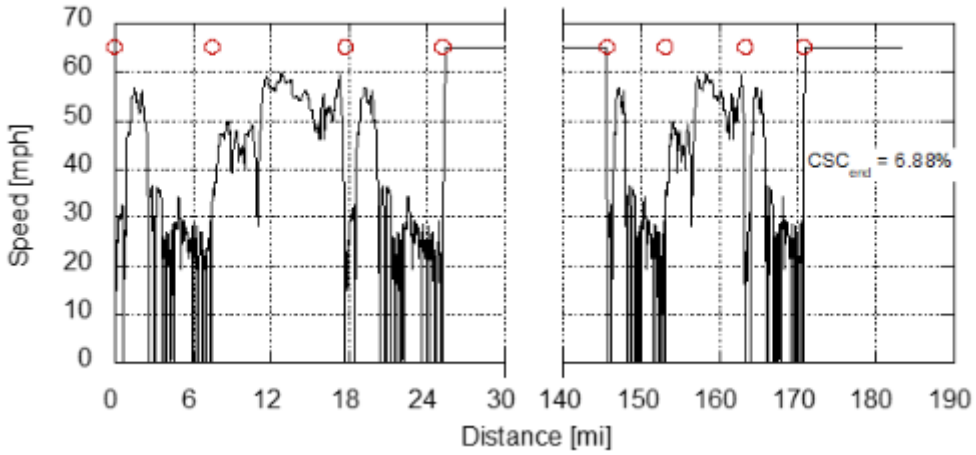

Figure 2.8: Created MCT cycle for the 2019 Chevy Bolt

The red circles on the graphs in Figure 2.8 correspond to the beginning and ending of the different components of the cycle (UDDS, HWFET, and CSC).

As a result of these considerations, the following methodology was taken when calibrating the model to EPA data:

1. Guessed a certain number of cycles based on the EPA stated range (i.e., cycles = 1000 mi/EPA range and rounded up) to find the corresponding capacity loss from Section 2.6.
2. Simulated the SAE J1634 test procedure and found the model parameters (e.g., auxiliary power draw and maximum SOC) that fit the EPA City and Highway range and miles per gallon equivalent (MPG_e) while ensuring the 20% or less requirement for the CSC at the end (CSC_{end}) was met (note: additional code was generated to dynamically create the MCT profile as indicated in Figure 2.8).
3. Calibrated the rolling resistance coefficients (a_{rr}, b_{rr}, and c_{rr} in Equation 2.19) to the EPA combined drag and rolling resistance model in Equation 2.2 from 0 to 100 miles per hour while calculating the individual drag force via Equation 2.4. Like other calibration efforts, the MATLAB *fmincon* optimization routine was utilized to minimize the difference between the two models.
4. Ran with the calibrated rolling resistance and drag information through the durability driving cycle routine over 1000 simulated miles to see if it altered the number of cycles from (a).
5. If it did change, (b) was redone using the new number of cycles and the procedure repeated.

At this point, the model was fully calibrated to the SAE J1634 test procedure.

Chapter 3: Results and Discussion

In Table A.1, all EV specifications and model parameters that were found (or guessed) are provided. In the following sections, the results of the model are described according to the influence of different parameters that affect their range.

3.1 SAE J1634 Results Including Vehicle Mass and Tire Pressure

Since the authors are not privy to the exact specifications of each vehicle and drivetrain (e.g., battery data and motor efficiency maps), while endeavoring to match the EPA stated ranges, it was decided that the maximum state of charge (SOC) of the battery pack be a calibration parameter. Investigating the representative batteries in Figure 2.3 through Figure 2.6, it was assumed that most EVs would not want to operate at a greater than 90% depth of discharge (10% SOC) since the voltage falls dramatically and the battery's chemistry can be damaged. For similar reasons, operating at greater than 80% SOC might not be preferred, with Kostopoulos et al. (2020) finding that most researchers suggest a 20-80% SOC range for reduced capacity degradation while maintaining a good cyclical performance. Generally, this assumption worked well with five of the vehicles demonstrating an SOC range from 0.1 to ~0.85. For the VW e-Golf, the SOC range had to be expanded to nearly the maximum to match EPA data. While this outcome is likely not realistic, concessions must be made when not all information is readily available. Overall, on average the model deviates from the EPA highway and city range by 0.45 and 0.57 miles, respectively, for the six vehicles simulated in Table A.1.

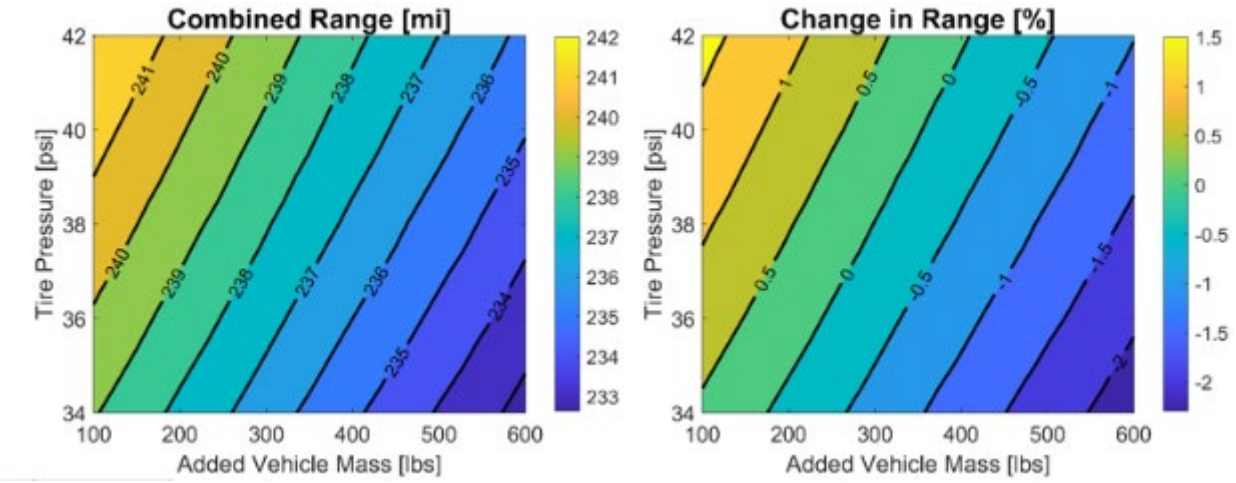

Figure 3.1: (Left) Combined Range and (Right) Percentage Change in Range for a Chevy Bolt Based on the Added Vehicle Mass and Tire Pressure

Figure 3.1 illustrates the influence of increased vehicle mass and tire pressure during a representative EPA test of the Chevy Bolt. As expected, adding vehicle mass reduces the range of the vehicle; albeit not dramatically, with around a 1-2% loss in range after doubling the added vehicle mass (300 lbs added is required in the SAE J1634 test procedure). Similarly, reducing the tire pressure finds a small corresponding loss in range of around 1% when the tire pressure is decreased by 2 psi. As stated before, the EPA test procedure is accomplished using a chassis dynamometer and does not include the influence of wind or road grade. In addition, it is accomplished without employing the HVAC system or even operating at most highway speed limits (i.e., its maximum speed is 65 mph as indicated in Figure 2.8); thus, it does not generally stress the battery pack. The respectively small losses according to added vehicle mass and tire pressure indicated in Figure 3.1 are likely under predicting what would be experienced in a real-world scenario.

3.2 Road Grade, Wind, and Vehicle Speed

As a test of real-world conditions, the Nissan Leaf model was simulated driving from Kansas City, Missouri (730.87 ft elevation) to the Colorado border (3847.77 ft elevation) along I-70 West at EPA test ambient conditions. Since the EPA test is performed at a maximum speed of 65 mph, immediately upon simulation of true highway speeds (note: GPS location data was

correlated to the posted speed limit) a Nissan Leaf loses 36.2% of its range without considering road grade and wind conditions as indicated in Figure 3.2. Subsequently, since traveling to the Colorado border has a respectively uphill grade, the vehicle now loses 37.2% of its EPA stated range when considering road elevation. In addition, in most months traveling west on I-70 encounters a wind force counter to vehicle motion; thus, adding in the negative impact of wind from June 2020 finds a 40.1% total range decrease. Finally, since a significant majority of drivers often drive faster than the posted speed limit (Mannering, 2007; De Leonardis et al., 2018; AAA Foundation for Traffic Safety, 2020), increasing the maximum speed of the vehicle to 80 mph (in the posted 75 mph speed limit zones), while factoring in wind and road grade demonstrates an overall 43.2% loss of EPA stated range.

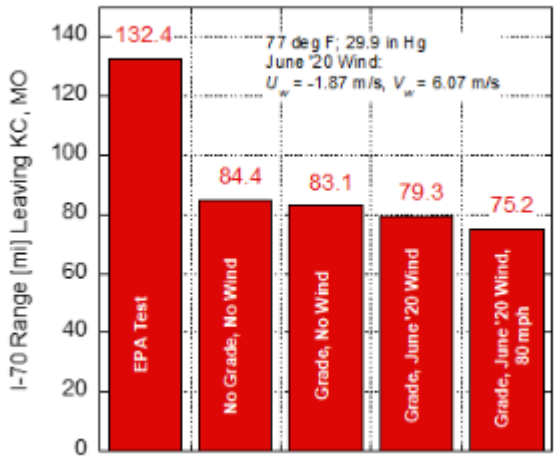

Figure 3.2: Illustration of Road Grade, Wind, and Vehicle Speed Influences on Range of Nissan Leaf at the EPA Tested Ambient Conditions

3.3 Ambient Temperature Conditions

To account for just the effect of different ambient temperatures, as discussed in Section 2.5, the α_{aux} parameter of Equation 2.34 was calibrated to the AAA data that provided reductions in driving range with the HVAC system off. Of note, AAA performed their tests according to the SAE J1634 methodology while including an additional driving cycle. This effort ignored the influence of this added driving cycle and simply utilized the respective losses in city and highway mileage

as a function of the two temperatures tested (20 °F and 95 °F) from AAA's base temperature data (75 °F). This was done for all vehicles where AAA data existed, and the other vehicles used an average value of α_{aux}. Overall, the model deviated from the experimental data by 1.90/3.53 and 4.78/3.03 miles for the city and highway ranges at 20 °F and 95 °F, respectively. Obviously, the losses due to ambient temperature conditions are more complex than what a single parameter can estimate; however, without more information about the vehicles, this simplistic model appears to provide a reasonable result.

Continuing the examination of a Nissan Leaf from the prior section, the respective range of this vehicle over the I-70 highway heading West was explored at the posted speed limits based on the ambient temperature. In Figure 3.3, the range of the vehicle is indicated before recharging is required when the HVAC system is *not* engaged; thus, each "leg" of the journey is provided based on the month of travel. Interestingly, a wide variance is seen as the wind direction changes from helping (December to February) to hurting (March to November). Overall, it would take five recharging stops to reach the Colorado border and possibly six when the wind direction is negatively influencing drag on the vehicle. In comparison, the EPA stated highway range predicts only three recharging events would be needed; thus, up to two times the amount of charging events might be encountered by the driver.

To account for the influence of the HVAC system engaged, the AAA data including the added effect of HVAC was utilized to determine the power draw parameters of Equations 2.35 and 2.36. Similarly, model calibration using the MATLAB *fmincon* function utilized the respective losses in city and highway mileage as a function of the two temperatures tested (20 °F and 95 °F) from their base temperature data. On average, at 20 °F the model deviates by 8.68 and 7.35 miles for the city and highway ranges, respectively; whereas, at 95 °F the model deviates by 2.83 and 2.90 miles, respectively, for the city and highway predictions. Ideally, more data points beyond two temperatures should be utilized to help calibrate the model (or fabricate a better model). However, the present model should still generate a respectively more realistic outcome under real world conditions than the SAE J1634 test procedure.

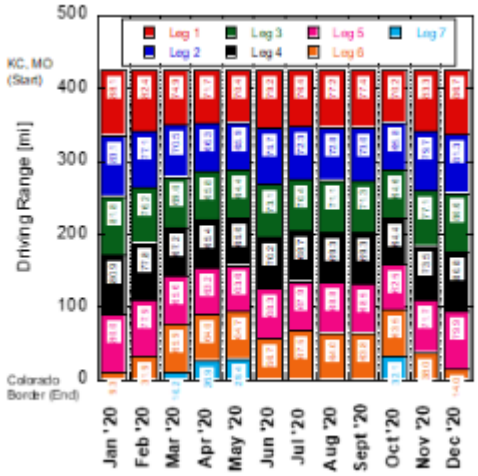

Figure 3.3: Traveling from Kansas City, MO to the Colorado Border on I-70 West with the Respective Range Indicated Before Charging is Necessary. HVAC System is Not Engaged

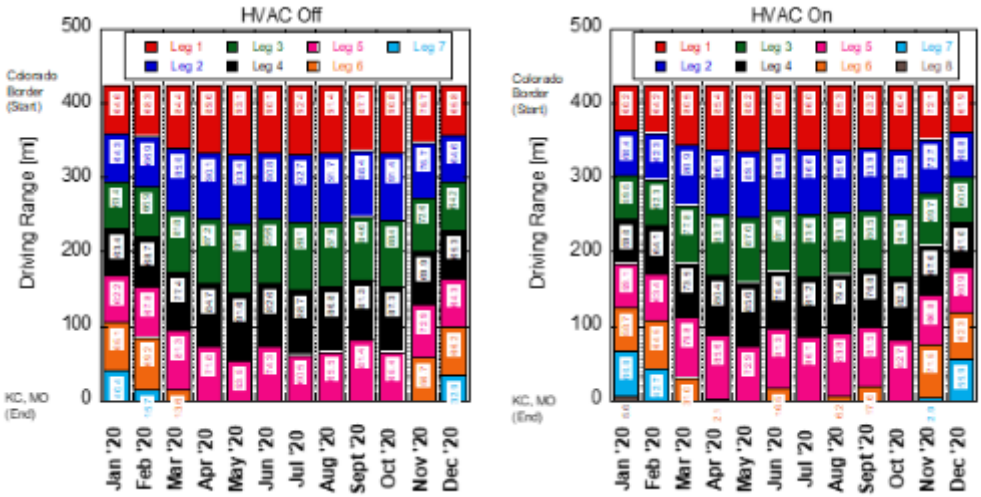

Figure 3.4: Traveling from the Colorado Border to Kansas City, MO on I-70 East with the (Left) HVAC System Off and (Right) HVAC System On

Figure 3.4 demonstrates the influence of engaging the HVAC system of the same vehicle (Nissan Leaf), but now driving from the Colorado border to Kansas City, MO, on I-70 East. Interestingly, using the January 2020 data finds that the vehicle now needs seven recharging events when the HVAC system is engaged. For this month, the respectively cold weather increases the requirements of the heating system with the greater density of air and negative impact of wind now increasing vehicle drag. On average for each leg that utilized the full *SOC* of the battery pack,

turning on the HVAC system lost around an additional 4.4 miles of range over the entire year. Compared to the EPA stated range of 132.4 miles, complete legs heading East on I-70 with its beneficial road grade had an average range of 75.1 miles (43.3% less) over the course of the year.

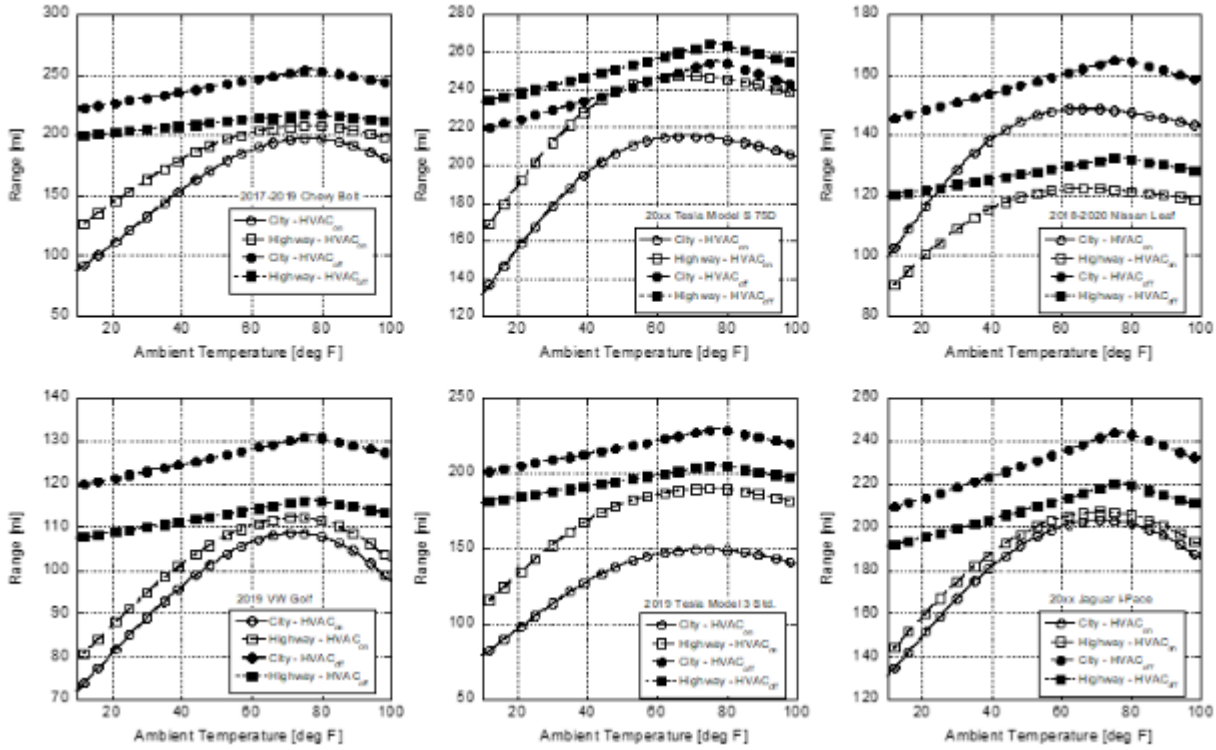

Figure 3.5: Range of the Different Modeled Vehicles Based on Ambient Temperature with the HVAC System Off (Solid Symbols) and HVAC System On (Open Symbols) Over the SAE J1634 Test Procedure

Figure 3.5 provides the modeled range of the vehicles for the SAE J1634 test procedure simulated as a function of ambient temperature and engagement of the HVAC system. Given the sparseness of data used for calibration, caution should be employed when using these models; however, the overall trend of range with ambient temperature follows the respective trend predicted by EV data (Argue, 2020). The Tesla Model 3 and Jaguar I-Pace HVAC on models were generated by scaling the respective average P_{aux} in Equation 2.36 using the vehicle cabin sizes (V_{cabin}) between the corresponding resistance heating (Chevy Bolt and Tesla Model S) and heat pump (Nissan Leaf and VW e-Golf) vehicles:

$$P_{aux,Model\,3} = F \cdot average\left(\frac{P_{aux,Bolt}}{V_{cabin,Bolt}}, \frac{P_{aux,Model\,S}}{V_{cabin,Model\,S}}\right) V_{Cabin,Model\,3}$$

Equation 3.1

While additionally determining a factor (*F*) that ensures the HVAC on model predicts at least 5% lower city and highway range than the corresponding HVAC off model for that vehicle at each temperature. The values in Table A.1 are the resulting parameters from these estimations.

As shown, the vehicles that employ a heat pump lose less range as a function of ambient temperature than the vehicles using resistance heaters. This is to be expected given the respective inefficiency of resistance heaters with heat pumps for EVs showing Coefficients of Performance around two (Bellocchi et al., 2018). Thus, more companies are investigating the potential of heat pumps while factoring in the additional cost required for this technology (Christen et al., 2017). Based on the Nissan Leaf and VW e-Golf losses, the use of scaling via Equation 3.1 first appears to overpredict the range loss for the Jaguar I-Pace. However, given the respective lower EPA range of these vehicles in comparison to the I-Pace, when normalized the percentage loss is relatively consistent: at 20 ºF. The Leaf and e-Golf lose 30.4% and 38.5% of their range, whereas the I-Pace is predicted to lose 38.8% of its range. Interestingly, Christen et al. (2017) found that Battery Electric Vehicles lose between about 30-50% of their range at 20 ºF and around 20% of their range at 95 ºF. The model predictions here indicate losses (city or highway) from 24.9-57.8% at 20 ºF to 8.1-37.5% at 95 ºF; thus, it appears the models generated here provide reasonable values.

3.4 Vehicle Age

As EVs age and the number of battery cycles undergone increases, Figure 2.7 demonstrates that the overall capacity of the battery pack will decrease. This could exacerbate the range anxiety of the consumer and possibly lead to the consumer returning to a petroleum-based vehicle. Interestingly, the accuracy of the predicted range of the vehicle was shown to account for around 20% of the satisfaction of an EV owner (McIntosh, 2021). Thus, it is important to understand how the range of an EV will change based on the driving location *and* the vehicle mileage.

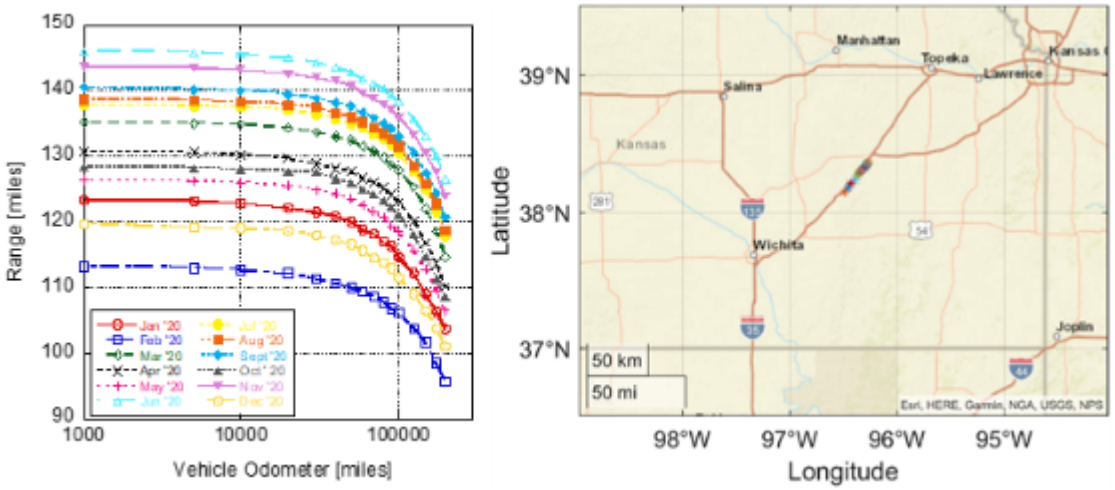

Figure 3.6: (Left) Range of Jaguar I-Pace on I-35 N Starting from the Oklahoma Border as a Function of the Time of Year and Number of Miles on the Odometer with the HVAC System Turned On. (Right) The Respective Stopping Points of the First Leg as the Vehicle Ages Using January 2020 as the Month

The left image in Figure 3.6 shows the range of the Jaguar I-Pace driving North on I-35 at different times of the year 2020 as the vehicle ages. The age of the vehicle was estimated by taking odometer mileage and dividing by the EPA stated combined range to determine the cycle to use with the models developed for Figure 2.7. This is likely an underestimation of the number of cycles but should provide sufficient insight. Again, each month shows a different range of the EV with the respective temperature and wind direction playing a role. Since the Jaguar is simulated using the NCM_{622} battery that has a respectively linear decrease in capacity with cycle usage, the range drops generally linearly with odometer mileage (shown here on a logarithmic x-axis). At around 90,000 miles, the vehicle has lost 5% of its range at that month and subsequent driving continues the loss up to around 15% at 200,000 miles. At 100,000 miles, the Jaguar averages 124.4 miles of range over the year, a respective 43.7% decrease over its EPA estimated 220.8 highway mile range, but only a 5.7% loss in range over its predicted range at 1000 miles.

The right image in Figure 3.6 demonstrates where the consumer would need to stop during the month of January as a function of vehicle age. As the odometer mileage increases, stops closer to Wichita, KS, would be needed. This could be problematic for the consumer if they are used to a particular stop location and do not pay attention to their EV losing range as it ages. It is also unknown whether each EV has its own factor in range projection that considers odometer mileage.

If not, it is possible the satisfaction of the consumer would subsequently decrease as the vehicle ages.

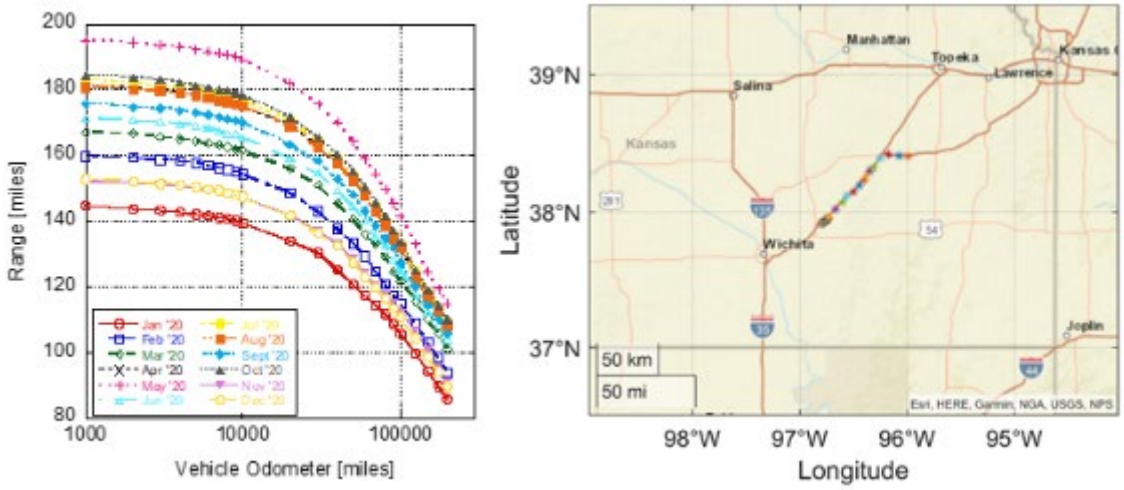

Figure 3.7: (Left) Range of Tesla Model S on I-35 S Starting from Kansas City, MO as a Function of the Time of Year and Number of Miles on the Odometer with the HVAC System Turned On. (Right) The Respective Stopping Points of the First Leg as the Vehicle Ages Using November 2020 as the Month

In comparison, the left image of Figure 3.7 illustrates that it only takes the Tesla Model S around 15,000 miles to lose 5% of its range and at 100,000 miles it has lost on average 28.1% of its initial range for that month. This result is due to the chosen NCA battery aging curve in Figure 2.7 having a more drastic loss in battery capacity with the number of battery cycles. This is assumed to be a function of the respective nickel level of the perceived battery chemistries. Adding nickel improves the overall capacity of the battery but leads to a proportional decrease in its performance during cycling (Park et al., 2019). Note that NCA batteries generally are of the $LiNi_{0.8}Co_{0.15}Al_{0.05}O_2$ chemistry and this also explains why the NCM_{523} battery performs better cyclically than the NCM_{622} battery in Figure 2.7.

Now, at 100,000 miles the average range over the year is 124.1 miles which is a respective 53.1% decrease over its EPA estimated 264.6 highway mile range. Furthermore, the right image of Figure 3.7 demonstrates a significant difference in stopping locations based on odometer mileage. In general, the layered ternary cathode materials of NCM and NCA batteries have a significantly high storage capacity and voltage potential making them suitable for long-range EVs;

however, they can have a poor rate capacity (Liu et al., 2020). Thus, as shown here, it is important to understand the impact of battery aging as it can lead to significant losses in EV range potentially exacerbating the range anxiety of the driver.

3.5 Rain and Snow

As indicated in the introduction, both rain and snow can lead to a respective increase in rolling resistance subsequently impacting the range of an EV. In addition, the prior sections investigated high-speed corridors through the state of Kansas. Given the squared factor of velocity impacting drag in Equation 2.4, this will result in a greater loss of range in comparison to a lower speed route. Thus, the left image in Figure 3.8 demonstrates the impact of rain on the range of a Tesla Model 3 during a respectively lower speed route (US-54 East). As indicated, the range of the vehicle falls generally linearly with the amount of rain on the road during July of 2020. Reviewing the stopping locations in the right image of Figure 3.8 finds, like age, that sooner stops are needed and at the highest rain level on the road (0.10 in.), a third stop would be required before reaching the Missouri border.

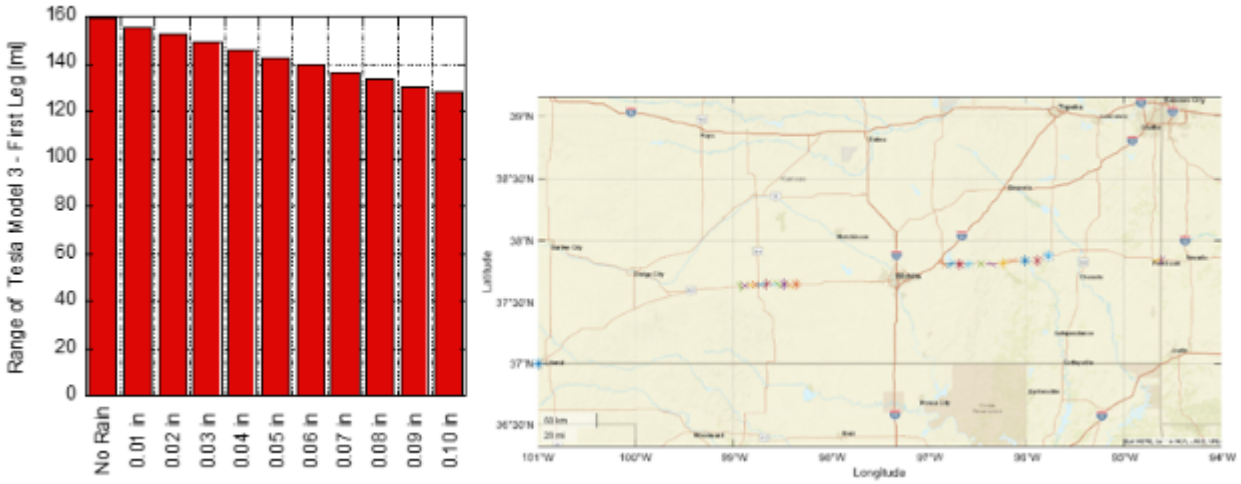

Figure 3.8: (Left) Range of Tesla Model 3 in July 2020 Heading East on US-54 as a Function of Rain on Road. (Right) Stopping Locations Based on Rain Level with Sooner Stops Needed Heading Out of Liberal, KS. Vehicle Mileage = 1000 miles, HVAC System On

With respect to snow, the left image in Figure 3.9 demonstrates the range of the Tesla Model 3 heading West on US-54 with varying levels of fresh snow on the ground in February 2020. Like rain, the range of the EV drops linearly with the amount of snow cover. Now, three stops are needed for all scenarios to make it from the Missouri border to Liberal, KS with snow having a relatively significant impact on range. Both the rain and snow results indicate that EVs might consider linking to local weather stations to obtain rainfall/snowfall data and modify their range predictions accordingly.

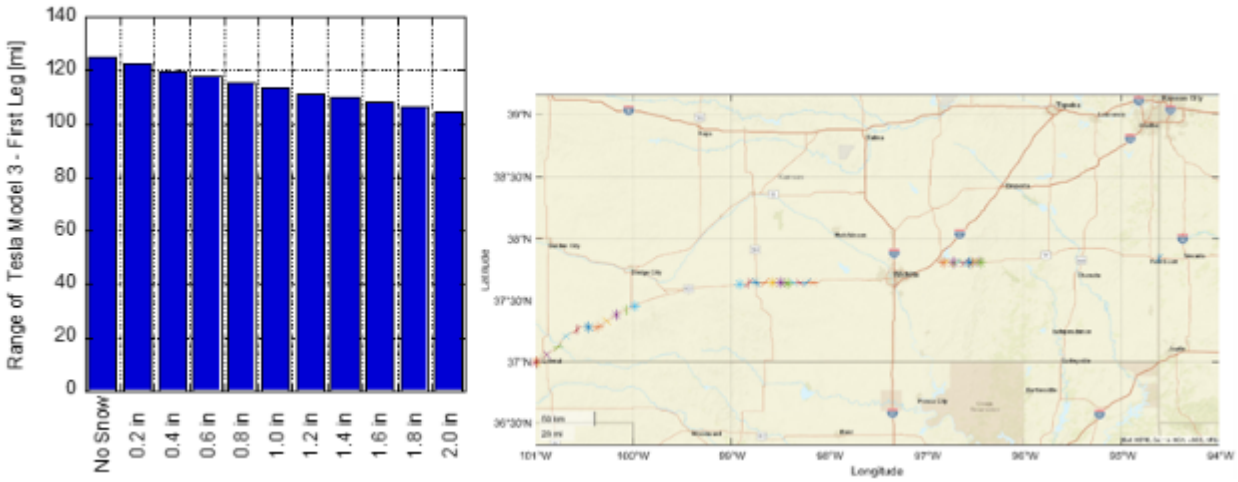

Figure 3.9: (Left) Range of Tesla Model 3 in February 2020 Heading West on US-54 as a Function of Snow on Road. (Right) Stopping Locations Based on Snow Level with Sooner Stops Needed Heading from the Missouri Border. Vehicle Mileage = 1000 miles, HVAC System On

3.6 Model Exploration

The constructed model is believed to be the simplest version that captures nearly all pertinent facets which impact EV driving range. As a final demonstration of its use, a vehicle comparison of the final state of charge driving on I-135 North and South is provided in Figure 3.10 during August of 2020 with the HVAC system engaged and the vehicle aged 50,000 miles. The total distance on this respectively short interstate route is 95.9 miles; hence, all vehicles as indicated by the EPA should be able to traverse this route without needing to stop. Furthermore, an illustration of the predictive capability of the model is provided by simulating the 2021 VW

ID.4 for which only EPA data exists currently. Like earlier efforts, the calibration procedure of the VW ID.4 with the HVAC system off was accomplished to endeavor to match the MCT test results from the EPA (see Figure 3.11). Then, the same procedure as the Tesla Model 3 was done to estimate the mileage of the vehicle as a function of ambient temperature with the HVAC system off and on. Similar to the VW Golf, the SOC_{min} and SOC_{max} had to be expanded to their maximum values to achieve close to the EPA stated ranges and MPG_e. The values do deviate more than the other models, likely due to the fact it employs newer battery technology (NCM_{712}) but was assumed here to have the NCM_{622} battery profiles given the unavailability of literature data.

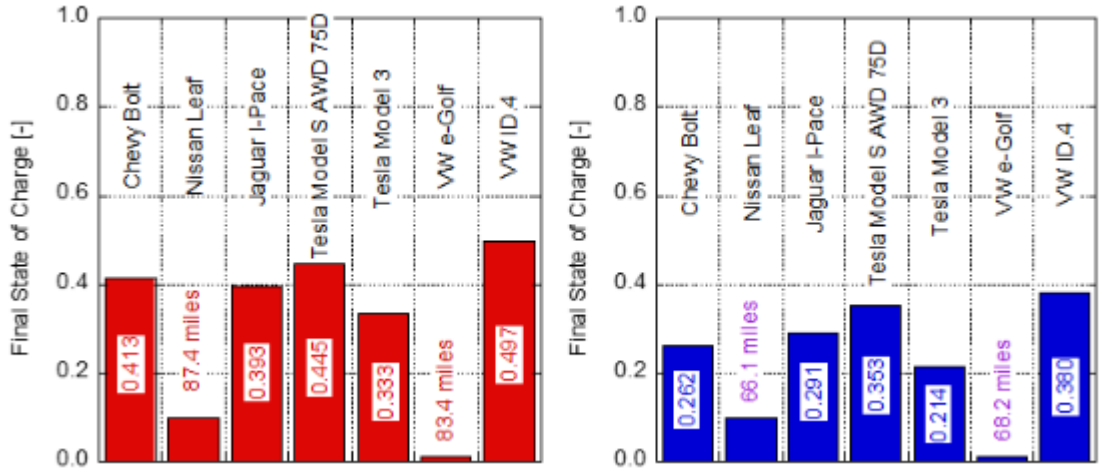

Figure 3.10: Final State of Charge of Each Vehicle or the Vehicle Range When Driving from (Left) Wichita, KS to Salina, KS or (Right) Salina, KS to Wichita, KS on I-135 North and South, Respectively, During August of 2020

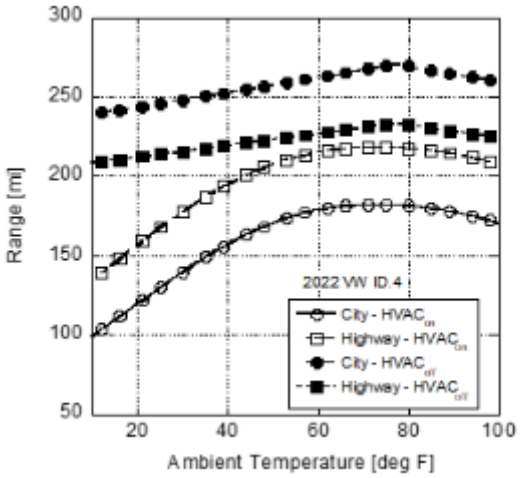

Figure 3.11: Estimated Range of the 2022 VW ID.4 Vehicle as a Function of Ambient Temperature with the HVAC System Off and On

As indicated in Figure 3.10, not all vehicles can make the I-135 trip without recharging. All vehicles will need recharging in Wichita, KS, to make the 191.8-mile roundtrip journey. Interestingly, the VW ID.4 has the best range likely given the fact it has been estimated with a newer battery chemistry. So, while battery technology continues to improve, it does seem that significant improvements are still needed to achieve the 300-mile range that has often been discussed as one barrier to commercial success (Andre et al., 2017). Finally, it would be interesting to check the predictability of the VW ID.4 model once more data are available.

3.7 Discussion and Recommendations

The findings illustrate that EPA should reconsider how they generate the range of EVs since range anxiety is a significant issue for the consumer. As illustrated, weather, speed, age of the vehicle, heating and air conditioning all play a large role in decreasing the range of EVs. Thus, data should be taken at different temperatures demonstrating the impact of the HVAC system. Moreover, a new driving profile more indicative of the speeds seen during highway driving is required. Furthermore, estimates of the loss of range based on whether it is raining or snowing, and the age of the vehicle should be provided to the consumer. It is critical that these advances in knowledge be portrayed to the consumer otherwise their attitudes towards EVs will change and they will revert to using petroleum-based vehicles. For example, about 20% of early adopters in

California have switched back with their dissatisfaction with home charging being a primary factor (Lane, 2021). The data illustrated here demonstrates that more charging events will be needed given current battery technology; thus, potentially exacerbating the dissatisfaction of consumers.

3.8 Predictive Spreadsheet

Given the relative complexity of the model for others to use and the need to translate the findings for widespread usage as part of planning purposes, it was decided to extrapolate the findings into an Excel spreadsheet. To generate the spreadsheet, the six vehicles in Table A.1 were simulated over the routes I-135, US-54, I-70, and I-35 in both directions over each month of the year 2020. In addition, the influence of vehicle age (through mileage: m_i), the HVAC system (off and on), and the amount of rain on the road (t_{rt}) was included as variable parameters. From this information, an average range multiplier (R_{mult}) across all vehicles was determined that can be used to modify the EPA stated range of the vehicle. After doing so, it was realized that the data could be coalesced into a curve-fit:

$$\boldsymbol{R_{mult} = (A + B \cdot t_{rt})\left(C + D \cdot m_i + E \cdot m_i^2 + F \cdot m_i \cdot t_{rt}\right)}$$

Equation 3.2

Using Matlab's *fmincon* function, the values of A, B, C, D, E, and F were fit to each route, whether the HVAC system was on or off, and the month of the year. In comparison to the model results, the curve-fit had around a 0.2% difference in R_{mult}.

Figure 3.12 illustrates the input to the spreadsheet along with the model results. All the user has to accomplish is to provide the EPA stated range of the vehicle, the level of charge of the battery pack, the current mileage of the vehicle, whether the HVAC system is engaged, and if there is rain on the road. The calibrated curve-fit will then tell the user what the estimated range of that vehicle will be over the routes provided.

Questions	Input to Model	
What is the EPA stated range of the vehicle?	213	miles
What is the current battery pack charge level (0% - Empty; 100% - Full)	87%	
What is the mileage (aka odometer) of the vehicle?	49,000	miles
Is the HVAC system ON or OFF?	ON	
How much rain is on the road in inches?	0.05	inches

	Estimated Electric Vehicle Range in Miles based on Road Speed, Direction, and Ambient Conditions							
	I-135 North	I-135 South	US-54 East	US-54 West	I-70 East	I-70 West	I-35 North	I-35 South
Jan.	83.5	87.6	111.5	85.4	98.7	75.6	85.9	78.5
Feb.	78.5	94.0	103.7	90.5	95.4	80.6	78.4	85.4
Mar.	103.7	79.4	107.5	107.4	86.8	94.7	94.0	89.0
Apr.	102.5	82.8	103.0	114.1	84.5	100.8	90.5	95.5
May	99.6	88.9	100.9	119.8	84.9	105.7	87.3	102.3
June	113.4	81.6	115.4	113.0	91.8	99.7	101.7	92.3
July	107.4	86.3	109.8	116.5	90.2	103.0	95.9	97.6
Aug.	107.6	86.2	110.9	115.6	91.0	102.1	96.5	96.7
Sept.	107.1	84.0	112.2	112.7	90.9	99.0	97.0	93.5
Oct.	101.7	83.4	101.4	115.5	83.5	102.1	89.2	97.0
Nov.	103.7	79.3	118.0	98.2	94.7	86.3	99.8	81.9
Dec.	80.9	92.3	109.8	87.7	99.3	77.8	82.6	82.1

Figure 3.12: (Top) Inputs to the Model; (Bottom) Corresponding Estimated Range Based on Route and Month of the Year

Chapter 4: Conclusions

Range anxiety continues to be a primary factor for consumers when considering the purchase of an EV. While numerous EVs now boast ranges greater than 200 miles based on EPA data generated from the SAE J1634 testing procedure, the actual range of the EV on-road can be significantly less. Weather, weight, road conditions and grade, along with cabin conditioning, all play a large role in decreasing actual driving distance. To account for these facets, this effort endeavored to create the simplest model that accounts for all pertinent factors to generate a more realistic outcome of EV range.

Initial calibration of six commercial vehicles to the EPA stated range data finds good accuracy with the model deviating by only 0.45 and 0.57 miles for the highway and city ranges, respectively. Of the six vehicles, five were estimated to have state of charge (*SOC*) ranges deemed suitable within research findings. Subsequently, predicting a Chevy Bolt in simulated chassis dynamometer tests finds only a 1-2% loss in range due to added weight or tire pressure. However, simulating the impact of road grade, wind, and vehicle speed over a true highway environment demonstrated significant losses up to 43.2% of the EPA stated range for a Nissan Leaf. In addition, ambient temperature effects resulted in the Leaf requiring around two times the amount of charging events. Overall, model predictions indicate losses (city or highway) from 24.9%-57.8% at 20 ºF to 8.1%-37.5% at 95 ºF for the vehicles simulated.

Battery chemistry was also found to play a role in EV range as the vehicle ages. The simulated Jaguar I-Pace with a NCM_{622} battery had a respective 43.7% decrease in range at 100,000 miles, whereas the Tesla Model S with a NCA battery predicted a 53.1% decrease in range at the same vehicle mileage. Here, the respectively greater decrease in capacity of the NCA battery with cycles resulted in the Tesla losing a larger percentage of its range with mileage. Subsequent model expansion that was employed to include rain and snow data demonstrates different stopping locations amongst a lower speed route that suggests in-vehicle estimations of range might need to link to local weather stations to modify their algorithms. Model exploration and expansion to the VW ID.4 finds significant efforts are still needed in battery chemistry to achieve a true 300-mile on-road range for lower cost EVs. It is recommended that the EPA reconsider their range

estimations and provide more realistic values expected by the consumer given possible driving profiles in Kansas based on the time of year and the age of the vehicle. Finally, a respectively simple spreadsheet was created that allows for users to quickly estimate the range of an electric vehicle based on route, time of the year, battery pack charge, age of the vehicle, whether the HVAC system is engaged, and if rain is present.

References

AAA Foundation for Traffic Safety. (2020). *2019 traffic safety culture index*. AAA Foundation for Traffic Safety. https://aaafoundation.org/wp-content/uploads/2020/06/2019-Traffic-Safety-Culture-Index.pdf

Ahn, Y., & Yeo, H. (2015). An analytical planning model to estimate the optimal density of charging stations for electric vehicles. *PLOS ONE, 10*(11), Article e0141307. https://doi.org/10.1371/journal.pone.0141307

Akçelik, R., & Besley, M. (2001). *Acceleration and deceleration models* [Paper presentation]. 23rd Conference of Australian Institutes of Transport Research (CAITR 2001), Monash University, Melbourne, Australia. https://www.researchgate.net/publication/238778191

Al-Wreikat, Y., Serrano, C., & Sodré, J. R. (2021). Driving behaviour and trip condition effects on the energy consumption of an electric vehicle under real-world driving. *Applied Energy, 297*, Article 117096. https://doi.org/10.1016/j.apenergy.2021.117096

American Association of State Highway and Transportation Officials. (2001). *A policy on geometric design of highways and streets* (4th ed.). American Association of State Highway and Transportation Officials.

American Automobile Association, Inc. (2019). *AAA electric vehicle range testing*. https://www.aaa.com/AAA/common/AAR/files/AAA-Electric-Vehicle-Range-Testing-Report.pdf

Andre, D., Hain, H., Lamp, P., Maglia, F., & Stiaszny, B. (2017). Future high-energy density anode materials from an automotive application perspective. *Journal of Materials Chemistry A, 5*(33): 17174-17198. https://doi.org/10.1039/C7TA03108D

Argue, C. (2020, May 25). *To what degree does temperature impact EV range?* Geotab. https://www.geotab.com/blog/ev-range/

Autolist Analytics Team. (2021, May 3). *Survey: Electric vehicles' range jumps to top of priorities for consumers*. Autolist. https://www.autolist.com/news-and-analysis/2021-survey-electric-vehicles

Bellocchi, S., Guizzi, G. L., Manno, M., Salvatori, M., & Zaccagnini, A. (2018). Reversible heat pump HVAC system with regenerative heat exchanger for electric vehicles: Analysis of its impact on driving range. *Applied Thermal Engineering, 129*, 290-305. https://doi.org/10.1016/j.applthermaleng.2017.10.020

Bennett, C. R., & Dunn, R. C. M. (1995). Driver deceleration behavior on a freeway in New Zealand. *Transportation Research Record, 1510*, 70-75. https://onlinepubs.trb.org/Onlinepubs/trr/1995/1510/1510-009.pdf

Bokare, P. S., & Maurya, A. K. (2017). Acceleration-deceleration behaviour of various vehicle types. *Transportation Research Procedia, 25*, 4733-4749. https://doi.org/10.1016/j.trpro.2017.05.486

Burress, T. (2013, May 14). *Benchmarking state-of-the-art technologies* [PowerPoint slides]. 2013 U.S. DOE Hydrogen and Fuel Cells Program and Vehicle Technologies Program Annual Merit Review and Peer Evaluation Meeting, Arlington, Virginia. https://www.energy.gov/sites/default/files/2014/03/f13/ape006_burress_2013_o.pdf

Christen, E. J., Blatchley, T., Jacobson, M., Ahmed, N. K., & Gong, Q. (2017). *Improving range robustness: Heat pump value for plug-in electric vehicles* (SAE Technical Paper No. 2017-01-1161). https://doi.org/10.4271/2017-01-1161

De Leonardis, D., Huey, R., & Green, J. (2018). *National traffic speeds survey III: 2015* (Report No. DOT HS 812 485). National Highway Traffic Safety Administration. https://doi.org/10.21949/1525935

Depcik, C., Gaire, A., Gray, J., Hall, Z., Maharjan, A., Pinto, D., & Prinsloo, A. (2019). Electrifying long-haul freight—Part II: Assessment of the battery capacity. *SAE International Journal of Commercial Vehicles, 12*(2), 87-102. https://doi.org/10.4271/02-12-02-0007

Durability Driving Schedules, 40 C.F.R. Appendix IV to Part 86 (2011). https://www.govinfo.gov/content/pkg/CFR-2011-title40-vol19/pdf/CFR-2011-title40-vol19-part86-appIV.pdf

Ejsmont, J., Sjögren, L., Świeczko-Żurek, B., & Ronowski, G. (2015). Influence of road wetness on tire-pavement rolling resistance. *Journal of Civil Engineering and Architecture, 9*(11), 1302-1310. http://dx.doi.org/10.17265/1934-7359/2015.11.004

Evtimov, I., Ivanov, R., & Sapundjiev, M. (2017). Energy consumption of auxiliary systems of electric cars. In B. Gigov, N. Nikolov, V. Stoilov, & M. Todorov (Eds.), *9th International Scientific Conference on Aeronautics, Automotive and Railway Engineering and Technologies (BulTrans-2017)*. (MATEC Web of Conferences 133, Article 06002). EDP Sciences. https://doi.org/10.1051/matecconf/201713306002

Fechtner, H., Teschner, T., & Schmuelling, B. (2015). Range prediction for electric vehicles: Real-time payload detection by tire pressure monitoring. In *2015 IEEE Intelligent Vehicles Symposium (IV)* (pp. 767-772). IEEE. https://doi.org/10.1109/IVS.2015.7225777

Grover, P. S. (1998). *Modeling of rolling resistance test data* (SAE Technical Paper No. 980251). https://doi.org/10.4271/980251

Hao, X., Wang, H., Lin, Z., & Ouyang, M. (2020). Seasonal effects on electric vehicle energy consumption and driving range: A case study on personal, taxi, and ridesharing vehicles. *Journal of Cleaner Production, 249*, Article 119403. https://doi.org/10.1016/j.jclepro.2019.119403

Hausmann, A., & Depcik, C. (2013). Expanding the Peukert equation for battery capacity modeling through inclusion of a temperature dependency. *Journal of Power Sources, 235*, 148-158. https://doi.org/10.1016/j.jpowsour.2013.01.174

Hausmann, A., & Depcik, C. (2014). A cost-effective alternative to moving floor wind tunnels in order to calculate rolling resistance and aerodynamic drag coefficients. *SAE International Journal of Passenger Cars - Mechanical Systems 7*(2): 703-713. https://doi.org/10.4271/2014-01-0620

Horrein, L., Bouscayrol, A., Lhomme, W., & Dépature, C. (2017). Impact of heating system on the range of an electric vehicle. *IEEE Transactions on Vehicular Technology, 66*(6): 4668-4677. https://doi.org/10.1109/TVT.2016.2615095

Idaho National Engineering Laboratory. (1996, January). *USABC electric vehicle battery test procedures manual: Revision 2* (Report No. DOE/ID-10479, Rev. 2). U.S. Department of Energy. https://doi.org/10.2172/214312

Kadijk, G., & Ligterink, N. (2012). *Road load determination of passenger cars* (TNO Report R10237). TNO. https://repository.tno.nl/SingleDoc?docId=34499

Kihlgren, B. (1977). *Flygplanshjuls rullmotstånd i torr nysnö* (VTI Report 128). Statens Väg- och Trafikinstitut. https://www.diva-portal.org/smash/get/diva2:674400/FULLTEXT01.pdf

Kleeman, P. T. (1998). *A fresh look at predicting carbon monoxide impacts at highway intersections* [Paper presentation]. Joint Summer Meeting of Transportation Research Board Committees A1F03 and A1F06, Ann Arbor, Michigan. https://web.archive.org/web/19991110122235/http://www.angelfire.com/va/pkleeman/trbpaper.html

Kostopoulos, E. D., Spyropoulos, G. C., & Kaldellis, J. K. (2020). Real-world study for the optimal charging of electric vehicles. *Energy Reports 6*, 418-426. https://doi.org/10.1016/j.egyr.2019.12.008

Kwon, S.-J., Lee, S.-E., Lim, J.-H., Choi, J., & Kim, J. (2018). Performance and life degradation characteristics analysis of NCM LIB for BESS. *Electronics, 7*(12), 406. https://doi.org/10.3390/electronics7120406

Lane, B. W. (2021). From early adopters to early quitters. *Nature Energy, 6*(5), 458-459. https://doi.org/10.1038/s41560-021-00836-3

Larsson, M. (2014). *Electric motors for vehicle propulsion* (Report No. LiTH-ISY-EX--14/4743—SE). Linköpings Universitet. https://urn.kb.se/resolve?urn=urn:nbn:se:liu:diva-103907

Laurikko, J., Granström, R., & Haakana, A. (2012). Assessing range and performance of electric vehicles in Nordic driving conditions – Project "RekkEVidde." *World Electric Vehicle Journal 5*(1), 45-50. https://doi.org/10.3390/wevj5010045

Lin, X., Harrington, J., Ciampitti, I., Gowda, P., Brown, D., & Kisekka, I. (2017). Kansas trends and changes in temperature, precipitation, drought, and frost-free days from the 1890s to 2015. *Journal of Contemporary Water Research & Education 162*(1), 18-30. https://doi.org/10.1111/j.1936-704X.2017.03257.x

Liu, K., Yamamoto, T., & Morikawa, T. (2017). Impact of road gradient on energy consumption of electric vehicles. *Transportation Research Part D: Transport and Environment, 54*, 74-81. https://doi.org/10.1016/j.trd.2017.05.005

Liu, L., Li, M., Chu, L., Jiang, B., Lin, R., Zhu, X., & Cao, G. (2020). Layered ternary metal oxides: Performance degradation mechanisms as cathodes, and design strategies for high-performance batteries. *Progress in Materials Science, 111*, Article 100655. https://doi.org/10.1016/j.pmatsci.2020.100655

Mannering, F. L. (2007). *The effects of interstate speed limits on driving speeds: Some new evidence* [Paper presentation]. 86th Annual Meeting of the Transportation Research Board, Washington, DC.

Maurya, A. K., & Bokare, P. S. (2012). Study of deceleration behaviour of different vehicle types. *International Journal for Traffic and Transport Engineering, 2*(3), 253-270. doi.org/10.7708/ijtte.2012.2(3).07

McIntosh, J. (2021, May) *Do people who buy their first electric vehicle buy a second one after?* Driving. https://driving.ca/auto-news/news/do-people-who-buy-their-first-electric-vehicle-buy-a-second-one-after

Momen, F., Rahman, K. M., Son, Y., & Savagian, P. (2016). Electric motor design of General Motors' Chevrolet Bolt electric vehicle. *SAE International Journal of Alternative Powertrains, 5*(2), 286-293. https://doi.org/10.4271/2016-01-1228

Mruzek, M., Gajdáč, I., Kučera, Ľ., & Barta, D. (2016). Analysis of parameters influencing electric vehicle range. *Procedia Engineering, 134*, 165-174. https://doi.org/10.1016/j.proeng.2016.01.056

National Centers for Environmental Information. (2021). *U.S. wind climatology*. National Oceanic and Atmospheric Administration. https://www.ncei.noaa.gov/access/monitoring/wind/

O'Malley, R., Liu, L., & Depcik, C. (2018). Comparative study of various cathodes for lithium ion batteries using an enhanced Peukert capacity model. *Journal of Power Sources, 396*, 621-631. https://doi.org/10.1016/j.jpowsour.2018.06.066

Panasonic. (2012). *Lithium Ion NCR18650B*. https://web.archive.org/web/20220809041938/https://www.batteryspace.com/prod-specs/NCR18650B.pdf

Park, K.-J., Hwang, J.-Y., Ryu, H.-H., Maglia, F., Kim, S.-J., Lamp, P., Yoon, C. S., & Sun, Y.-K. (2019). Degradation mechanism of Ni-enriched NCA cathode for lithium batteries: Are microcracks really critical? *ACS Energy Letters, 4*(6), 1394-1400. https://doi.org/10.1021/acsenergylett.9b00733

Pavlat, J. W., & Diller, R. W. (1993). An energy management system to improve electric vehicle range and performance. *IEEE Aerospace and Electronic Systems Magazine, 8*(6), 3-5. https://doi.org/10.1109/62.216890

Pevec, D., Babic, J., Carvalho, A., Ghiassi-Farrokhfal, Y., Ketter, W., & Podobnik, V. (2020). A survey-based assessment of how existing and potential electric vehicle owners perceive range anxiety. *Journal of Cleaner Production, 276*, Article 122779. https://doi.org/10.1016/j.jclepro.2020.122779

Proctor, C. L., Grimes, W. D., Fournier Jr, D. J., Rigol Jr, J., & Sunseri, M. G. (1995). *Analysis of acceleration in passenger cars and heavy trucks* (SAE Technical Paper 950136). https://doi.org/10.4271/950136

Prša, A., Harmanec, P., Torres, G., Mamajek, E., Asplund, M., Capitaine, N., Christensen-Dalsgaard, J., Depagne, É., Haberreiter, M., Hekker, S., Hilton, J., Kopp, G., Kostov, V., Kurtz, D. W., Laskar, J., Mason, B. D., Milone, E. F., Montgomery, M., Richards, M., … Stewart, S. G. (2016). Nominal values for selected solar and planetary quantities: IAU 2015 resolution B3. *The Astronomical Journal, 152*(2), Article 41. https://dx.doi.org/10.3847/0004-6256/152/2/41

SAE J1634. (2017, July). *Battery electric vehicle energy consumption and range test procedure*. SAE International. https://doi.org/10.4271/J1634_201707

Samadani, E., Fraser, R., & Fowler, M. (2014). *Evaluation of air conditioning impact on the electric vehicle range and Li-ion battery life* (SAE Technical Paper No. 2014-01-1853). https://doi.org/10.4271/2014-01-1853

Samenow, J. (2016, March 31). Blowing hard: The windiest time of year and other fun facts on wind. *Washington Post*. https://www.washingtonpost.com/news/capital-weather-gang/wp/2014/03/26/what-are-the-windiest-states-and-cities-what-is-d-c-s-windiest-month/

Samsung. (2015, December 31). *Introduction of Samsung SDI's 94 Ah cells* [PowerPoint slides]. https://files.gwl.eu/inc/_doc/attach/StoItem/7213/Samsung_SDI_94Ah_Datasheet.pdf

Sarrafan, K., Muttaqi, K. M., Sutanto, D., & Town, G. E. (2018). A real-time range indicator for EVs using web-based environmental data and sensorless estimation of regenerative braking power. *IEEE Transactions on Vehicular Technology, 67*(6), 4743-4756. https://doi.org/10.1109/TVT.2018.2829728

Sarrafan, K., Sutanto, D., Muttaqi, K. M., & Town, G. (2017). Accurate range estimation for an electric vehicle including changing environmental conditions and traction system efficiency. *IET Electrical Systems in Transportation, 7*(2), 117-124. https://doi.org/10.1049/iet-est.2015.0052

Saxena, S., Le Floch, C., MacDonald, J., & Moura, S. (2015). Quantifying EV battery end-of-life through analysis of travel needs with vehicle powertrain models. *Journal of Power Sources, 282*, 265-276. https://doi.org/10.1016/j.jpowsour.2015.01.072

Sinnott, R. W. (1984). Virtues of the haversine. *Sky and Telescope, 68*(2), 158.

SketchAndCalc. (n.d.). *Area calculator*. Accessed on June 1, 2022. https://www.sketchandcalc.com/area-calculator/

Staton, D., & Goss, J. (2017). *Open source electric motor models for commercial EV & hybrid traction motors* [PowerPoint slides]. Coil Winding, Insulation & Electrical Manufacturing Exhibition (CWIEME), Berlin, Germany. https://web.archive.org/web/20190730211639/https://www.coilwindingexpo.com/berlin/__media/pages/Tutorial-1-D--Staton-&-J--Goss-MDL.PDF

Szumska, E. M., & Jurecki, R. S. (2021). Parameters influencing on electric vehicle range. *Energies, 14*(16), Article 4821. https://doi.org/10.3390/en14164821

Tang, L., Wei, S., Valentage, J., Li, Z., & Nair, S. (2020, October 7). *Tire pressure impact on EV driving range*. SAE International. https://www.sae.org/news/2020/10/tire-pressure-impact-on-ev-driving-range

Tannahill, V. R., Muttaqi, K. M., & Sutanto, D. (2016). Driver alerting system using range estimation of electric vehicles in real time under dynamically varying environmental conditions. *IET Electrical Systems in Transportation, 6*(2), 107-116. https://doi.org/10.1049/iet-est.2014.0067

U.S. Department of Energy & U.S. Environmental Protection Agency. (2021). *Download fuel economy data*. Available online: https://www.fueleconomy.gov/feg/download.shtml

U.S. Environmental Protection Agency. (n.d.). *Data on cars used for testing fuel economy*. Accessed on September 21, 2021. https://www.epa.gov/compliance-and-fuel-economy-data/data-cars-used-testing-fuel-economy

Voelcker, J. (2017, August 24). *How much electric-car range is 'enough'? 300 miles much better than 200 miles: Survey*. Green Car Reports. https://www.greencarreports.com/news/1112298_how-much-electric-car-range-is-enough-300-miles-much-better-than-200-miles-survey

Wang, J., Dixon, K. K., Li, H., & Ogle, J. (2005). Normal deceleration behavior of passenger vehicles at stop sign–controlled intersections evaluated with in-vehicle Global Positioning System data. *Transportation Research Record, 1937*, 120-127. https://doi.org/10.1177/0361198105193700117

Weiss, M., Cloos, K. C., & Helmers, E. (2020). Energy efficiency trade-offs in small to large electric vehicles. *Environmental Sciences Europe, 32*, Article 46. https://doi.org/10.1186/s12302-020-00307-8

Yi, Z., & Bauer, P. H. (2017). Effects of environmental factors on electric vehicle energy consumption: A sensitivity analysis. *IET Electrical Systems in Transportation, 7*(1), 3-13. https://doi.org/10.1049/iet-est.2016.0011

Yuksel, T., & Michalek, J. J. (2015). Effects of regional temperature on electric vehicle efficiency, range, and emissions in the United States. *Environmental Science & Technology, 49*(6), 3974-3980. https://doi.org/10.1021/es505621s

ZeroAir Reviews. (2018, November 13). *LiionWholesale Samsung 50e 21700 Li-ion cell review*. https://zeroair.org/2018/11/13/liionwholesale-samsung-50e-21700-li-ion-cell-review

Appendix

Table A.1: Pertinent Vehicle Parameters for Six Commercial EVs

Vehicle and Model Year	2017-2019 Chevy Bolt	2018-2020 Nissan Leaf	2019 Jaguar I-Pace	2019 Tesla Model S AWD 75D	2019 Tesla Model 3 Std. Range RWD	2019 VW e-Golf
AAA Test Data Available	Yes	Yes	No	Yes	No	Yes
Coefficient of Drag [-]	0.32	0.28	0.29	0.24	0.23	0.25
Vehicle Height [in]	62.8	61.6	61.3	56.5	56.8	58.3
Vehicle Width [in]	69.5	70.5	74.6	77.3	72.8	70.8
Frontal Area [ft^2]	23.80	23.27	24.92	21.81	21.36	22.04
Vehicle Mass [lbm]	3563	3433	4718	4883	3552	3494
Unloaded Tire Diameter [in]	25.5	24.9	29.6	27.7	29.4	24.9
Tire pressure [psi]	38	36	37	45	37	41
Tire Revolutions per Mile [rev/min]	815	836	703	751	708	836
Final Drive Ratio [-]	7.05	8.19	9.06	9.73	9	9.75
Motor Type	Permanent Magnet Synchronous A	Permanent Magnet Synchronous B	Permanent Magnet Synchronous B	AC Induction	Permanent Magnet Synchronous B	Permanent Magnet Synchronous B
Maximum Motor Speed [rpm]	8810	10390	13000	18000	13800	12000
Maximum Brake Torque [ft-lbf]	266	237	513	485	318	214
Maximum Brake Power [hp]	201	148	397	518	283	134
Maximum Regeneration Power [hp]	80	58	156*	80	156*	94
Maximum Speed [mph]	91	89.5	124	139.8	130	93.2

Cabin Volume [ft^3]	94.4	116.0	102.6	94	97	93.5
Battery Chemistry [-]	NCM_{622}	NCM_{523}	NCM_{622}	NCA_1	NCA_2	NCM
Batteries in Series [-]	96	96	108	96	96	88
Batteries in Parallel [-]	3	2	4	74	46	3
Nominal Pack Voltage [VDC]	350	350	388	400	350	370
Nominal Pack Capacity [Ah]	171.4	115	222.9	245	230	111
Calculated Pack Capacity [lbm ft^2/s^2]	5.125E+09	3.439E+09	7.389E+09	8.372E+09	6.877E+09	3.509E+09
Initial Cycles for EPA Tests [-]	4	6	4	6	4	8
SOC_{min} / SOC_{max}	0.1 / 0.8305	0.1 / 0.9071	0.1 / 0.8664	0.1 / 0.8298	0.1 / 0.8571	0.01 / 0.9946
EPA City/Highway [mi]	255.1 / 217.4	165.2 / 132.4	244.8 / 220.8	255.0 / 264.6	230.5 / 206.3	130.6 / 117.9
Model City/Highway [mi]	254.6 / 218.0	165.3 / 132.5	244.8 / 220.7	255.6 / 265.1	229.6 / 205.7	131.2 / 116.4
Unadjusted MPG_e City/Highway	182.2 / 157.4	177.3 / 142.1	114.1 / 102.9	137.9 / 142.7	138.2 / 123.8	126.0 / 111.0
Model MPG_e City/Highway	182.9 / 156.6	177.3 / 142.1	114.1 / 102.9	137.9 / 143.0	138.2 / 123.8	125.7 / 111.5
HVAC Off 20°F & 95°F City/Highway Loss [mi]	-31 / -15 -6 / -2	-19 / -9 -2 / -2	N/A	-32 / -21 -19 / -14	N/A	-13 / -3 -7 / 0
HVAC Off Model 20°F & 95°F City/Highway Loss [mi]	-28.6 / -16.2 -9.4 / -5.1	-17.3 / -10.9 -5.6 / -3.5	-31.4 / -25.5 -10.6 / -8.5	-31.5 / -27.3 -10.6 / -9.0	-24.8 / 21.4 -8.2 / -7.0	-10.0 / -7.7 -3.3 / -2.5
HVAC On 20°F & 95°F City/Highway Loss [mi]	-148 / -68 -65 / -22	-58 / -26 -24 / -8	N/A	-109 / -69 -48 / -25	N/A	-65 / -20 -34 / -9

HVAC On Model 20°F & 95°F City/Highway Loss [mi]	-145.1 / -74.5 -69.5 / -17.6	-50.3 / -33.0 -21.2 / -13.3	-95.1 / -62.2 -53.8 / -24.5	-99.4 / -75.7 -48.2 / -25.1	-132.8 / -86.1 -86.1 / -20.8	-50.5 / -29.2 -30.2 / -10.8
$C_{r,mult}$	1.0428	1.0596	1.0428	0.9045	0.9884	0.9012
γ	0.8786	0.9222	0.8786	0.8851	1.0069	0.8861
χ	1.0391	1.0592	1.0391	1.0095	1.0552	1.0042
δ**	0	0	0	1.7714	0	0.4936
a_{EPA} [lbf]	14.2	8.330	-13.983	-1.500	17.400	-6.205
b_{EPA} [lbm/s]	0.8863	2.7705	6.1906	0.2582	-3.2752	0.9998
c_{EPA} [lbm/ft]	0.2889	0.2887	0.2760	0.2332	0.2455	0.2594
a_{rr} [lbf]	1.1278E-02	6.7031E-03	-8.6277E-03	-9.5951E-04	1.3725E-02	-5.1430E-03
b_{rr} [lbm/s]	7.0409E-04	2.2298E-03	3.8197E-03	1.6215E-04	-2.5798E-03	8.2834E-04
c_{rr} [lbm/ft]	5.9856E-06	3.8527E-05	5.5655E-06	2.5502E-05	5.0418E-05	4.622E-05
a_{aux} [hp] – HVAC off	1.2940	8.3547E-01	2.0130	2.4572	1.6177	4.9124E-01
b_{aux} [lbf] – HVAC off	13.740	16.165	33.002	32.937	1.330	89.535
c_{aux} [lbm/s] – HVAC off	3.4225	8.0910	22.904	8.8994	25.611	2.22097
α_{aux} – HVAC off	2.3446E+00	2.2228E+00	1.8577E+00	1.6729E+00	1.8577E+00	1.0136E+00
Heating System	Resistance	Heat Pump	Heat Pump	Resistance	Resistance	Heat Pump
a_{aux} [hp] – HVAC on	4.1808E-02	8.4216E-03	8.2343E-03	2.3231E-02	1.8047E-02	1.3332E-02
b_{aux} [lbf] – HVAC on	1.3783E-01	1.6164E-01	7.7890E-02	3.0929E-01	1.4173E-01	9.7108E-02
c_{aux} [lbm/s] – HVAC on	2.0025E-02	8.0028E-02	4.9161E-02	2.9624E-02	1.5192E-02	6.9020E-02
a_{YM} [lbm ft/s^2]	2.1176E+03	2.2330E+03	6.5384E+03	2.3234E+03	5.3000E+03	3.9608E+03
b_{YM} [lbf/°F]	-1.797	-1.750	-3.774	-1.641	-4.087	-1.886
c_{YM} [lbf/°F^2]	2.3476E-02	2.5647E-02	4.8066E-02	2.3895E-02	5.6207E-02	2.1592E-02
d_{YM} [lbf/°F^3]	-1.2331E-04	-1.4232E-04	-2.5094E-04	-1.3689E-04	-3.0495E-04	-1.1497E-04
e_{YM} [lbf/°F^4]	1.6666E-08	7.2918E-08	1.5045E-07	1.3822E-07	1.3924E-07	1.6276E-07
f_{YM} [lbf/°F^5]	2.0054E-09	1.4282E-09	4.0901E-09	1.0707E-09	3.7868E-09	2.2958E-09

*Guesses

Table A.2: Parameters for the 2021 VW ID.4

Coefficient of Drag [-]	0.28
Vehicle Height [in]	64.4
Vehicle Width [in]	72.9
Frontal Area [ft^2]	30.2*
Vehicle Mass [lbm]	4517
Unloaded Tire Diameter [in]	29.2
Tire pressure [psi]	50
Tire Revolutions per Mile [rev/min]	692
Final Drive Ratio [-]	12.99
Motor Type	Permanent Magnet Synchronous B
Maximum Motor Speed [rpm]	16000
Maximum Brake Torque [lbm ft^2/s^2]	7333
Maximum Brake Power [hp]	201
Maximum Regeneration Power [hp]	94*
Maximum Speed [mph]	99.4
Cabin Volume [ft^3]	99.9
Battery Chemistry [-]	NCM_{712} (used NCM_{622} data)
Batteries in Series [-]	96
Batteries in Parallel [-]	3
Nominal Pack Voltage [VDC]	400
Nominal Pack Capacity [Ah]	205
Calculated Pack Capacity [lbm ft^2/s^2]	7.005E+09
Initial Cycles for EPA Tests [-]	4
SOC_{min} / SOC_{max}	0.1 / 0.9999
EPA City/Highway [mi]	278.5 / 237.1
Model City/Highway [mi]	270.8 / 233.4
Unadjusted MPG_e City/Highway	107 / 91
Model MPG_e City/Highway	120.8 / 104.1
HVAC Off 20°F & 95°F City/Highway Loss [mi]	N/A
HVAC Off Model 20°F & 95°F City/Highway Loss [mi]	-27.7 / -21.4 -9.0 / -6.6
HVAC On 20°F & 95°F City/Highway Loss [mi]	N/A
HVAC On Model 20°F	-151.0 / -76.4

& 95°F City/Highway Loss [mi]	-96.4 / -22.2
$C_{r,mult}$	1.0428
γ	0.8786
χ	1.0391
δ	0
a_{EPA} [lbf]	14.635
b_{EPA} [lbm/s]	4.1103
c_{EPA} [lbm/ft]	0.2734
a_{rr} [lbf]	1.0410E-02
b_{rr} [lbm/s]	2.9202E-03
c_{rr} [lbm/ft]	2.1735E-05
a_{aux} [hp] – HVAC off	1.8738
b_{aux} [lbf] – HVAC off	1.8039E-01
c_{aux} [lbm/s] – HVAC off	27.249
α_{aux} – HVAC off	1.8577E+00
Heating System	Resistance
a_{aux} [hp] – HVAC on	1.3329E-02
b_{aux} [lbf] – HVAC on	1.0478E-01
c_{aux} [lbm/s] – HVAC on	1.1198E-02
a_{YM} [lbm ft/s^2]	7.6684E+03
b_{YM} [lbf/°F]	-5.9129
c_{YM} [lbf/°F^2]	8.1301E-02
d_{YM} [lbf/°F^3]	-4.4093E-04
e_{YM} [lbf/°F^4]	1.9642E-07
f_{YM} [lbf/°F^5]	5.5121E-09

K-TRAN

KANSAS TRANSPORTATION RESEARCH AND NEW-DEVELOPMENT PROGRAM

AD ASTRA PER ASPERA

Kansas

Department of Transportation